EXTERNAL ROUGHNESS EFFECTS ON THE MEAN WIND PRESSURE DISTRIBUTION ON HYPERBOLIC COOLING TOWERS

by

Cesar Farell and Federico E. Maisch

Sponsored by

National Science Foundation
Grant No. G.K. 35795

and

The Marley Company
Mission, Kansas

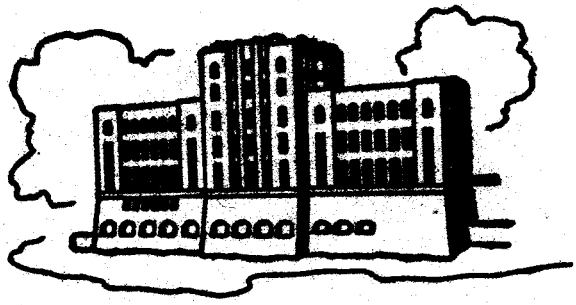

IIHR Report No. 164

Iowa Institute of Hydraulic Research
The University of Iowa
Iowa City, Iowa

August, 1974

EXTERNAL ROUGHNESS EFFECTS ON THE MEAN WIND PRESSURE DISTRIBUTION ON HYPERBOLIC COOLING TOWERS

by

Cesar Farell and Federico E. Maisch

Sponsored by

National Science Foundation
Grant No. G.K. 35795

and

The Marley Company
Mission, Kansas

IIHR Report No. 164

Iowa Institute of Hydraulic Research
The University of Iowa
Iowa City, Iowa

August, 1974

ABSTRACT

The effect of external, concentrated roughness elements or ribs on the mean pressure distributions on model hyperbolic cooling towers in uniform wind was experimentally investigated in the 5-foot low-turbulence wind tunnel of the IIHR. Several longitudinal rib configurations were tested, varying systematically rib height, rib width, and rib spacing. Three uniformly distributed, or random, roughnesses were also tested for purposes of comparison. Independence of the Reynolds number was achieved in the model experiments with the larger relative roughnesses. The base-pressure coefficient was found to be fairly constant along the height of the cooling tower model and independent of the relative roughness in the range of Reynolds number independence. On the other hand, the magnitude of the negative pressures on the sides of the model was found to depend markedly in this range of Reynolds numbers on the geometric characteristics of the roughness.

ACKNOWLEDGEMENTS

This study was sponsored by the National Science Foundation, under Grant No. G.K. 35795, and by The Marley Company, Mission, Kansas. Support for computer time was provided by the Graduate College of The University of Iowa. The advice of Mr. O. Güven and Professor V.C. Patel during various phases of this study is gratefully acknowledged.

TABLE OF CONTENTS

		Page
	LIST OF FIGURES	iv
	LIST OF TABLES	v
	LIST OF SYMBOLS	vi
I.	INTRODUCTION	1
II.	DIMENSIONAL ANALYSIS AND LITERATURE REVIEW	2
	A. Dimensional analysis	2
	B. Literature review	3
III.	EXPERIMENTAL EQUIPMENT AND PROCEDURE	9
	A. Model	9
	B. Wind tunnel	12
	C. Roughness	15
	D. Mean pressure data acquisition	16
	E. Data reduction procedure	18
IV.	RESULTS AND DISCUSSION	18
	A. Presentation of results	18
	B. Estimate of errors in the minimum pressure coefficient due to nonuniformities in the rib height k	28
	C. Influence of the width-to-height ratio of the ribs	28
	D. Influence of the ratio s/k	29
	E. Influence of the rib height	30
	F. Comparison of the results of the present study with results obtained by Niemann (1971)	31
	G. Comparison of the effect of concentrated and distributed roughnesses	33
	H. Interference effects between ribs and pressure taps	34
	J. Characterization of a pressure distribution	35
V.	CONCLUSIONS	40
	LIST OF REFERENCES	43
	APPENDIX A: TABLES	45

LIST OF FIGURES

		Page
Fig. 1.	Minimum pressure coefficient as a function of relative roughness in the range of Reynolds number independence. For rib roughnesses, the value of the parameter s/k is given next to each point.	4
Fig. 2.	Prototype and model dimensions. Model scale: 1/250. Mean model diameter: 8.27 in.	11
Fig. 3.	Cooling tower model with 52 ribs ($k/d = 3.99 \times 10^{-3}$, $b/k = 1.97$)	13
Fig. 4.	Cooling tower model without ribs in the wind tunnel looking from upstream	14
Fig. 5.	Scheme of data acquisition system for the mean pressure distributions	17
Fig. 6.	Mean pressure distribution on smooth model	20
Fig. 7.	Mean pressure distribution for one of the rib configurations investigated	21
Fig. 8.	Average mean pressure distributions for different roughness configurations	22
Fig. 9.	Minimum pressure coefficient as a function of Reynolds number for the rib patterns investigated	23
Fig. 10.	Base pressure coefficient as a function of Reynolds number for the rib patterns investigated. Symbols as in Fig. 9.	24
Fig. 11.	Minimum and base pressure coefficients as functions of relative height along the tower for the smooth model. - - - - -: with air flow through the model ($U' = 0.25U$), $Re = 4.7 \times 10^5$; ————: without air flow through the model, $Re = 4.8 \times 10^5$	26
Fig. 12.	Minimum and mean pressure coefficients as functions of relative height along the tower for the roughness configurations investigated. - - - - -: with air flow through the model ($U'/U = 0.25$); ————: without air flow through the model.	27
Fig. 13.	Comparison of Niemann's results (in dashed lines) with results obtained in the present study. (Results for ribbed models are for 52 ribs.)	32
Fig. 14.	Zero crossing of the pressure distribution as a function of the pressure minimum. - - - - -: Niemann (1971)	37
Fig. 15.	Correlation between position of the pressure minimum and its magnitude. - - - - -: Niemann (1971)	38
Fig. 16.	Correlation between beginning of dead water region, θ_N, and pressure-distribution characteristic value $\min Cp - Cp_N$. - - - - -: Niemann (1971)	39

LIST OF TABLES

		Page
Table A-1.	Literature review	46
Table A-2.	Roughness characteristics	50
Table A-3.	Summary of tests	51

LIST OF SYMBOLS

b	rib width
Cp	pressure coefficient
Cp_N	base pressure coefficient
d	mean diameter of cooling tower
d_t	diameter at throat of tower
h	elevation above ground level
H	cooling tower height
k	rib height
ℓ	vertical distance measured from the model waist
ℓ_1	distance from top to waist of tower
ℓ_2	distance from top of tower to measuring cross section
min Cp	minimum pressure coefficient
p	pressure at angular distance θ from the forward stagnation point on the structure
p_0	static pressure in the undisturbed stream
Re	Reynolds number ($=Ud/\nu$)
s	circumferential center-to-center distance between ribs at throat of tower.
U	velocity of uniform stream
U'	velocity of air flow through the tower
x,y	profile coordinates
ν	kinematic viscosity
ρ	mass density
θ_0	angular position of zero crossing of the pressure distribution
θ_1	angle at which min Cp occurs
θ_N	angle at which separation occurs

EXTERNAL ROUGHNESS EFFECTS ON THE MEAN WIND PRESSURE DISTRIBUTION ON HYPERBOLIC COOLING TOWERS

I. INTRODUCTION

An understanding of surface roughness effects on the characteristics of the flow around cooling tower shells is essential for their structural design. Indeed, model tests on cooling towers have disclosed that external roughness elements - either uniformly distributed random-shaped elements or geometrically regular configurations of ribs or strakes - significantly reduce the magnitude of the negative pressures on the sides of the model and, very likely, also the intensity of the pressure fluctuations. Such elements are therefore favorable from a design standpoint if they can be shown to have a similar effect on prototype towers. The physical mechanisms responsible for the surface roughness effects, however, have not yet been satisfactorily elucidated (see, e.g., Farell 1971), and the applicability of the model results to prototype structures, for which the Reynolds numbers are generally two to three orders of magnitude greater than the model Reynolds numbers, is somewhat uncertain. Indeed, satisfactory modeling criteria for wind-tunnel studies of the wind loading on cooling towers (and, more generally, on large rounded structures), though very much needed for proper interpretation of wind-tunnel results, are not available at present.

The net result of the foregoing considerations is considerable divergence in practice regarding use of surface strakes to reduce the pressure loadings on natural draft cooling towers. Cooling towers constructed in Europe, especially those in Germany, are fitted generally with small external strakes which, incidentally, are also used to support slip forms during construction. The prototype tower at Weisweiler investigated by Niemann (1971), for example, has 52 ribs, 1.8 cm. high and 8 cm. wide, spaced at uniform intervals around the tower. Some American designers (see, e.g., Rogers and Cohen 1970) favor the use of ribs while others have not adopted them.

The work reported herein is part of a wider research program which has as primary objectives the understanding of the physical mechanisms responsible for the observed surface roughness effects, the elucidation of the modeling problem, and the model testing of different roughness configurations to ascertain their relative merits for use on prototype structures. The primary purpose of this particular study was to investigate the effect of external, concentrated roughness elements or ribs on the mean pressure distribution on model hyperbolic cooling towers in uniform wind, in the region of Reynolds number independence. Several longitudinal rib configurations were tested, systematically varying rib height, rib width, and rib spacing. Two uniformly distributed, or random, roughnesses were also tested for purposes of comparison. Furthermore, the present data has been compared with other available experimental information, and the physical mechanisms responsible for the observed effects have been discussed qualitatively so as to support extension of the appropriate model results to prototype conditions.

II. DIMENSIONAL ANALYSIS AND LITERATURE REVIEW

A. Dimensional Analysis. An understanding of the parameters relevant to the problem can be obtained by dimensional analysis. For models with longitudinal ribs, one obtains for the pressure coefficient $Cp = (p-p_o)/(\rho U^2/2)$ the expression

$$Cp = f(\theta, Ud/\nu, k/d, s/k, b/k, h/H, \text{tower shape, tunnel blockage})$$

where p is the mean pressure at an angular distance θ from the forward stagnation point on the structure; p_o is the static pressure in the oncoming undisturbed stream of uniform velocity U, mass density ρ, and kinematic viscosity ν; d is the mean diameter of the structure; k is the height, and b the width, of the ribs; s is the circumferential center-to-center distance between ribs at the throat of the tower; H is the height of the tower; and h is the elevation of each section above ground level. The free-stream turbulence intensity is assumed to be negligible. For models with distributed roughness the expression is the same except that the parameters s/k and b/k should be replaced by parameters representative of the grain packing and size distribution. For large enough values of the Reynolds number, $Re = Ud/\nu$,

the coefficient Cp becomes independent of Re. In this zone of Reynolds number independence any characteristic parameter of the pressure distribution can be plotted as a function of the geometric characteristics of the rib pattern. One often-used parameter is the minimum value of the pressure coefficient at a section slightly below the throat of a tower. This parameter (denoted by min Cp) is used in the next section to present a comparison of data obtained by various authors.

B. Literature Review. Figure 1 shows values of the minimum pressure coefficient, min Cp, plotted versus values of the relative roughness height, k/d, taken from published experimental investigations as discussed below. (The points obtained in the present investigation are also shown.) For the rib roughnesses, the value of the parameter s/k is indicated next to each point; the value of the parameter b/k is not shown because it is assumed that there is very little, if any, influence of this parameter on the mean pressure distributions for all practical values of it (for which there is no interaction between the flow patterns around consecutive ribs). The values of min Cp reported correspond to sections slightly below the throat of the towers, chosen as best as possible as suggested by the tower aspect ratios and shapes to provide a basis for comparison. All points in Fig. 1 are considered to be in the region of Reynolds number independence on the basis of experimental results of Niemann and the present study regarding Reynolds number effects (a similar Reynolds number effect on the minimum pressure coefficient is assumed for concentrated and distributed roughnesses). Experiments with circular cylinders have been included in Fig. 1 only for cylinders of small aspect ratio, H/d, presenting a free end to the flow, so as to resemble the flow over the top of a cooling tower. Table A-1 gives some relevant information about each investigation. The Reynolds number values reported are based upon the mean diameters of models and prototypes. A brief review of the investigations follows.

As early as 1930, Dryden and Hill investigated external roughness effects upon mean wind pressure distributions. They tested in the open air an experimental stack 30 ft. high and 10 ft. in diameter. The surface of the stack was covered by metal sheets nailed to a frame. Assuming the absolute roughness provided by the nails to be about 0.03 in., we have k/d =

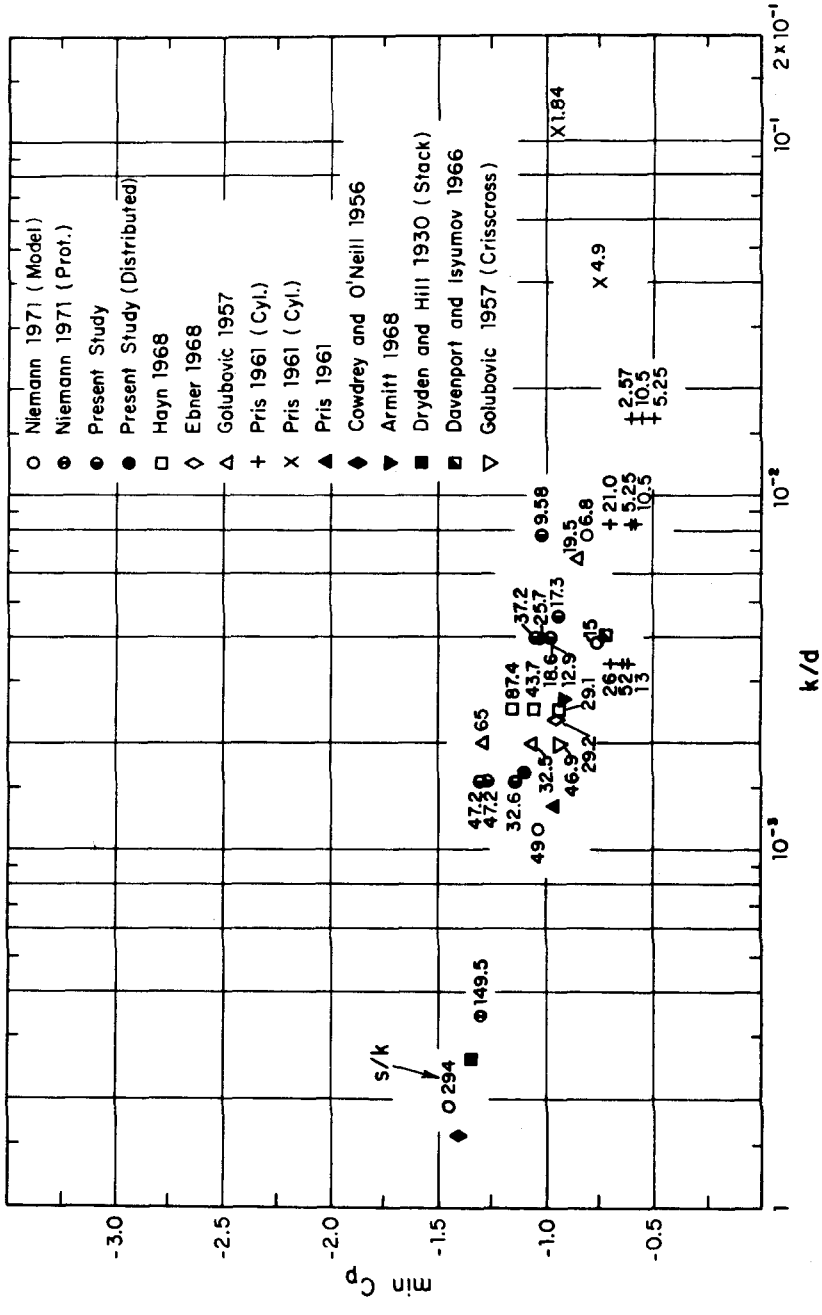

Fig. 1. Minimum pressure coefficient as a function of relative roughness in the range of Reynolds number independence. For rib roughnesses, the value of the parameter s/k is given next to each point.

2.6×10^{-4}. The value of min Cp reported is about -1.35 for a range of Reynolds numbers from approximately 2.5×10^{6} to 4.7×10^{6}. In 1956, Cowdrey and O'Neill carried out experiments for Reynolds numbers equal to 9.3×10^{6} and 14.1×10^{6}; they used a model cooling tower about 1.25 ft. in mean diameter, constructed of steel plate, in the form of a cylindrical throat and two truncated cones. Measurements were made both in a wind stream with a vertical velocity gradient (leaving an air inlet around the base of the tower open) and in a uniform wind stream (inlet closed). Only the results of the latter are plotted in Fig. 1. Assuming the roughness of the steel plate to be 0.0002 ft., $k/d = 1.2 \times 10^{-4}$, and the measured value of min Cp was -1.41. The pressure distributions were practically the same for both Reynolds numbers investigated. The research was carried out in the compressed air tunnel of the National Physical Laboratory in England which has an open test section 6 ft. in diameter. The horizontal blockage estimated as the ratio of model mean diameter to test section diameter was about 20.8%; the vertical blockage defined as the ratio of the height of the model to the height of the test section was about 27/66 = 40.9%.

Golubovic (1957) tested a model of a hyperbolic cooling tower for six different rib patterns at Reynolds numbers of the order of 10^{5}. In order to express the characteristics of the mean pressure distributions as functions of k/d and s/k, certain assumptions about the dimensions of the model must be made, since they are not given in the paper. For a Reynolds number of the order of 10^{5}, assuming for the kinematic viscosity a value of 1.5×10^{-5} $m.^{2}/sec.$, the product Ud is of the order of 1.5 $m.^{2}/sec.$ Under these conditions a mean diameter of 0.15 m. appears to be reasonable. The diameter at the waist can then be estimated as 0.13 m. Golubovic's results have been plotted in Fig. 1 on the basis of these assumptions.

Golubovic reports also tests conducted with ribs disposed along the two families of generators of the hyperboloid, for which he obtained min Cp = -0.93 for $k/d = 20 \times 10^{-4}$ and s/k = 49.6 (s is now the pitch of either family at the throat). Although Golubovic's results fit the general trend in Fig. 1, it should be kept in mind that the abcissa values may be in some error. Furthermore, no estimate of the blockage is available for these tests, although presumably it is not too large in view of the small model size estimated.

Pris (1961) carried out experiments using two circular cylinder fitted with ribs of two different widths in a wind tunnel with a cross sectional diameter of 2.0 m. One of the cylinders was 300 mm. in diameter and 400 mm. long (H/d = 4/3) and the ribs of three different heights. For these three heights the experiments were conducted at a Reynolds number of 6×10^5, with the cylinder suspended in the center of the wind tunnel. The pressure distribution was measured along the middle section. Comparison of these results with the others in Fig. 1 is made difficult by the small length-to-diameter ratio of the cylinders and the fact that they were suspended in the center of the tunnel.

The second cylinder had a diameter of 150 mm. and was tested at $Re = 3 \times 10^5$. This cylinder was 600 mm. long (H/d = 4) and was also suspended in the center of the tunnel. The ribs were much larger, 6 mm. wide and of two different heights, and the results suggest interference effects between the flow patterns about consecutive ribs. The vertical blockage, however, was somewhat larger for this cylinder, and this should account at least in part for the larger maximum suction. (The blockages in Table A-1 are estimated as the ratios of cylinder diameter and cylinder height to test section diameter.)

Pris (1959) also tested a hyperbolic cooling tower model 339 mm. in mean diameter for a Reynolds number of the order of 6.4×10^5. The horizontal blockage estimated as the ratio of mean model diameter to test section diameter was about 17%; the vertical blockage can be estimated (depending on the location of the false floor, which is not given) as 0.525/1.50 = 35%. Sawdust grains were used to obtain a random roughness on the model. Assuming 0.45 mm. as the average height of the grains, we have $k/d = 13.3 \times 10^{-4}$. The minimum pressure coefficient was -0.974.

Davenport and Isyumov (1966) experimented with both rigid and aero-elastic models of a hyperbolic cooling tower. Tests were carried out in turbulent boundary layers generated by covering the wind tunnel floor upstream from the model with appropriate roughness elements, as well as in uniform flows with different background turbulence levels. The boundary-layer wind tunnel of the University of Western Ontario has a test section 80 ft. long with a rectangular cross section 8 ft. wide and 7 ft. high.

A 1:300 model, vented at the base, and a 1:200 model, with the base sealed, of the Fort Martin cooling tower in West Virginia, were used.

The results for the smaller model placed in a uniform flow with 0.5% background turbulence are of interest here because three distributed roughnesses were investigated. This 1:300 model was 15.1 in. high and 8.1 in. in mean diameter (horizontal blockage 8.45%, vertical blockage 18.0%). No Reynolds number is given for these experiments. We will assume they were performed at Re = 1.94×10^5, the highest reported when studying the influence of Reynolds number upon the pressure distribution for the smooth model in the same uniform flow. The pressure distribution was measured at the throat of the model. For $k/d = 4 \times 10^{-4}$ (corresponding to $k/d_t = 5 \times 10^{-3}$, where d_t is the diameter at the throat) min. $C_p = -0.72$. (On the basis of Niemann's and the present results, the value of min. Cp at the throat and at a section corresponding to the measuring cross section chosen for comparison of results in Fig. 1 can be considered to be the same.)

Hayn (1967) measured mean pressure distributions for three different rib patterns on a model of one of the hyperbolic cooling towers of the Scholven power plant in Germany. The Reynolds number was 9.6×10^5 and the longitudinal ribs had relative height $k/d = 25 \times 10^{-4}$ (with $b/k = 2$). Three different rib spacings were tested. His results show that the absolute value of min Cp increases with increasing value of s/k but the variations are small. The horizontal blockage defined as the ratio of model mean diameter to wind tunnel width was 6.2%; the vertical blockage can be estimated as 25.2%, on the basis of the position of the platform (on which the model was mounted) as shown in Fig. 8 of Hayn's report. The platform used for the single tower experiments was only 1.0 m. by 1.0 m. and may be somewhat small to ensure the proper boundary conditions for the experiment.

Some odd results are presented by Paduart (1968) who made experiments with cylinders 1.50 m. high and 0.30 m. in diameter at a Reynolds number of 6.2×10^5. Paduart's results show min Cp = -1.00 for $k/d = 3.33 \times 10^{-4}$ and $s/k = 70$, and min Cp = -0.80 for $k/d = 7.33 \times 10^{-4}$ and $s/k = 45.5$.

Although this trend is in agreement with other available experimental information, the absolute values of min Cp are much lower than those obtained in the other experiments. Only very succinct information is given by Paduart regarding his experimental setup. But the cylinder was apparently not rigidly supported, a fact that becomes especially important in this case because the cylinder had an aspect ratio of 5 and spanned more than half of the tunnel cross section if allowance is made for the supporting platform. For this reason the results are not plotted in Fig. 1.

Armitt (1968) studied the effects of varying distributed roughness, free stream turbulence and Reynolds number on the mean pressure distribution on model cooling towers. The models used in his investigation were geometrically identical to the model used by Cowdrey and O'Neill (1956). For a Reynolds number of 4.87×10^5 and a turbulence level of 0.3%, Armitt tested three relative roughness heights. Only the roughness with k/d = 26.7×10^{-4}, for which min Cp = -0.92, is in the region of Reynolds number independence, and is plotted in Fig. 1. Although the horizontal blockage was fairly low, 8.3%, the vertical blockage was high, 43.6%.

Ebner (1968) made experiments for a model (mean diameter 0.211 m., height 0.407 m.) of the hyperbolic cooling tower of the power plant at Mengede, Germany, at a Reynolds number equal to 6.4×10^5. For a k/d value of 23.7×10^{-4} (b/k = 2.0) and s/k = 29, Ebner reports values of min Cp equal to -0.663, -0.761, -0.940, and -0.920 for relative heights, h/H, equal respectively to 0.788, 0.614, 0.442, and 0.271. The effect of the top of the tower upon the measurements at the two upper levels seems to be rather large for this particular model shape. For this reason the pressure distribution on the third level has been used for purposes of comparison with other measurements. Both horizontal and vertical blockages were high. The wind tunnel had an octagonal test section 2 m. long and 1.10 m. in mean diameter. The horizontal blockage was then about 0.211/1.10 = 19.2%. The vertical blockage can be estimated as 0.407/0.75 = 54% taking into account the location of the platform supporting the model, as shown in Fig. 2 of the report.

Niemann (1971) modeled a cooling tower built in 1966 in Weisweiler near Aachen, Germany, at a scale of 1:200. The model was 526 mm. high, had

a mean diameter of 262 mm. and was fitted with 52 equally-spaced vertical ribs (rib spacing 6.92°). The wind tunnel was almost rectangular in cross section, 5 m. high and 7 m. wide. Both horizontal and vertical blockages were therefore low, 3.7% and 12.7%, respectively.

In addition to the min Cp values corresponding to experiments in the region of Reynolds number independence, we have plotted in Fig. 1 a value obtained by extrapolation into that region of the curve depicting the variation of min Cp with Reynolds number that Niemann obtained for k/d = 1.92×10^{-4}. This k/d value is of interest because it is of the order of magnitude of the relative height of the concrete joints on some prototype shells. The extrapolated min Cp is -1.39, with s/k = 294, but can only be considered as a very rough estimate.

In spite of the difference in blockage ratios (the effects of which are treated at length by Farell, Carrasquel, and Maisch (1974)), which must be corrected before an accurate comparison can be made of the data in Fig. 1, and despite the fairly different shapes of the models used by different investigators, it is evident from Fig. 1 that the available data shows a marked decrease in mean suction with increasing relative roughness. (This trend may be reversed for very large relative rib heights due to interaction between the flow patterns around consecutive ribs, as will be discussed later in this report.) It also appears from Fig. 1 that the magnitude of the maximum suction decreases with decreasing relative rib spacing, s/k. This effect is not large and seems to be smaller for the larger k/d values. These conclusions will be discussed in more detail later in this report in the light of the results to be presented and a physical explanation for the trends will be given.

III. EXPERIMENTAL EQUIPMENT AND PROCEDURE

A. Model. A scale model of the hyperbolic cooling tower built in 1966 in Weisweiler, near Aachen, Germany, was selected for the study to provide for direct comparison with the results of Niemann's (1971) prototype and model investigations.

The equation for the profile of the Weisweiler tower as furnished by Niemann is

$$x^2/(22.30)^2 - y^2/(53.75)^2 = 1 \qquad (1)$$

(dimensions for Eq. 1 are in meters). The scale of the model constructed in the IIHR shop was 1:250 and the equation of the model's profile (values in inches) is therefore

$$x^2/(3.512)^2 - y^2/(8.465)^2 = 1 \qquad (2)$$

A computer program which solved Eq. 2 for x as a function of y provided the coordinates from which the profile of the model could be turned on a lathe. The model was cut in wood and was not vented at the base. Its mean diameter was 8.27 in. and its total height 16.55 in. Four measuring cross sections (referred to herein as sections A, B, C and D) were chosen at levels corresponding to relative heights, h/H, of 0.975, 0.823, 0.595, and 0.302, respectively, where H is the height of the tower and h is the elevation of each section above ground level. Cross sections A, B, and D correspond to measuring cross sections 1, 3, and 6 of Niemann's model. Section C corresponds to the measuring cross section in Niemann's prototype. Contrary to the statement in Niemann's report, measuring cross section 4 of his model is 5.97 m. (in prototype dimensions) higher than the prototype measuring cross section. This difference does not significantly affect the comparison between his model and prototype results; for the present study, however, section C has been chosen to correspond to the prototype measuring cross section, and is therefore somewhat lower than measuring cross section 4 in Niemann's model. Figure 2 shows the dimensions of model and prototype and the location of the measuring cross sections.

On the basis of the argument that the pressure distribution at levels just below the throat of a tower resembles somewhat (except for the wake suction) that corresponding to two-dimensional flow about a circular cylinder (see, e.g., Armitt 1968), a level in this region is frequently taken by investigators as a main source of data for analysis and conclusions. Therefore the model used in this investigation has a higher concentration of pressure taps at measuring cross section C, located at a relative distance, ℓ/H, below the throat of the tower equal to 0.143. (Furthermore, this cross section corresponds to the measuring cross section of the Weisweiler prototype tower).

Actually, two identical models were built, which permitted continuous operation of the wind tunnel during changes of the different rib

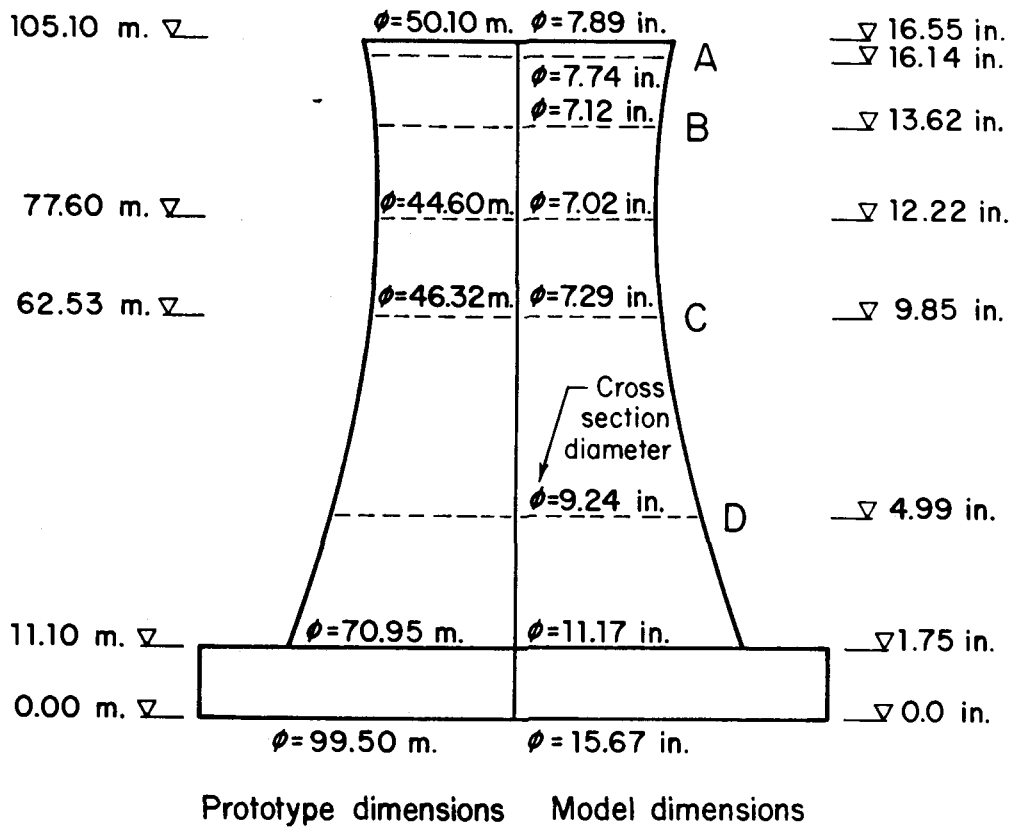

Fig. 2. Prototype and model dimensions. Model scale: 1/250. Mean model diameter: 8.27 in.

patterns investigated. For the model with 36 (or 18) equally-spaced ribs, the four sections contain a total of 108 pressure taps. Section C contains 30, located every 10° around the section excluding angles of ±40°, ±150°, and ±170°, for which no pressure taps were considered necessary. Sections A, B, and D contain 26 pressure taps, also located every 10° around each section, excluding those at angular positions ±20°, ±140°, ±160°, and ±170°. For the model with 52 (or 26) equally spaced ribs, the total number of pressure taps is 138. Section C contains 42 taps, located every 6.92° around the section excluding angles of ±20.8°, ±34.6°, ±48.5°, ±152.3°, and ±166.2°. Sections A, B, and D contain 32 pressure taps, also located every 6.92° around each section excluding those at angular positions ±13.8°, ±20.8°, ±34.6°, ±48.5°, ±62.3°, ±131.5°, ±145.4°, ±152.3°, ±166.2°, and ±173.1°. Figure 3 shows the cooling tower model fitted with one of the 52-rib configurations tested.

The pressure taps were made by drilling holes through the shell of the model tower and installing hypodermic needles with one end flush with the tower surface. The inside diameter of the needles was 0.046 in., which prevented dust from obstructing holes. This size for the inside diameter of the pressure taps produces an insignificant positive error in the pressure readings (Shaw 1960). The needles penetrated almost 0.5 in. inside the tower. Plastic tubing with an inside diameter of 0.063 in. was used to connect the taps to the recording devices to be described later. The tubing was tightly fitted and glued to prevent leaks.

B. Wind tunnel. The experiments were carried out in the largest closed-type low turbulence wind tunnel of the IIHR. An additional contraction and a corresponding diffuser have been added to the 24-ft.-long working section of the tunnel to change the original 5-ft. octagonal cross section to a rectangular cross section 5 ft. wide and 2.74 ft. high, the working section being now 9.5 ft. long. Figure 4 shows the upstream transition as well as the model, without ribs, in the test section, and gives a visual idea of the blockages, horizontal and vertical, which were respectively 13.9% and 50.4%.

In order to investigate the uniformity of the approach velocity distribution, measurements at a section 5.11 model mean diameters (42.25

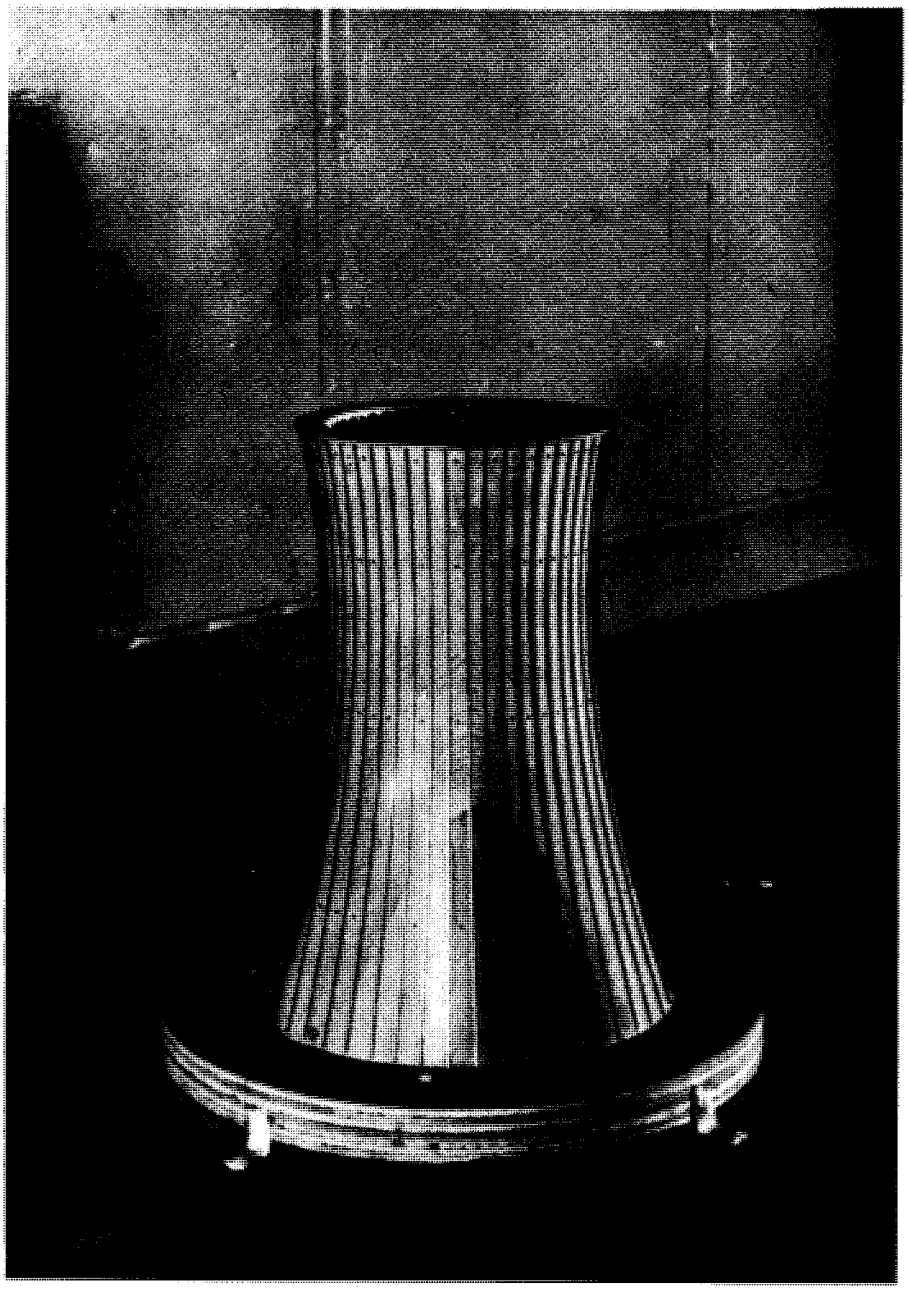

Fig. 3. Cooling tower model with 52 ribs ($k/d = 3.99 \times 10^{-3}$, $b/k = 1.97$)

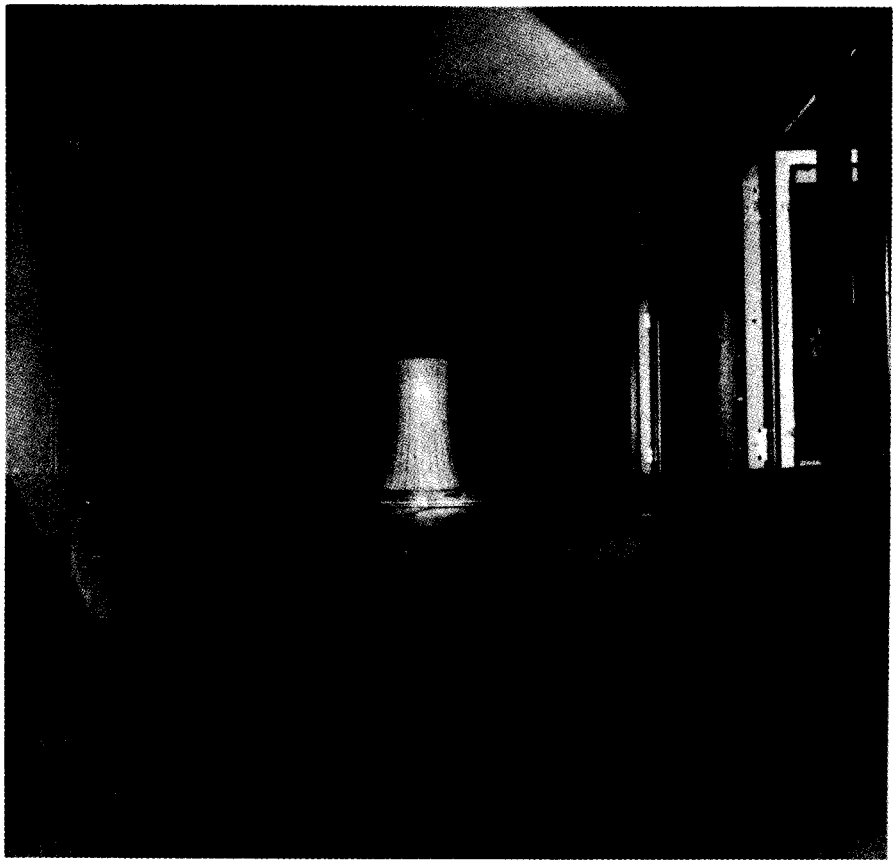

Fig. 4. Cooling tower model with 52 ribs in the wind tunnel looking from upstream

in.) upstream from the model axis were taken at four different levels. These levels were located at 4.43 in., 9.43 in., 16.43 in., and 23.43 in. respectively above the tunnel floor. (The distances from the tunnel floor to the four model measuring cross sections, A. B. C and D, are 16.14 in., 13.62 in., 9.85 in. and 4.99 in., respectively. The velocity distribution of the approach flow was reasonably uniform (with variations in the square of the velocity of at most 2% over the area investigated), as required for the present study. The background turbulence level was approximately 0.2%.

In order to locate a point at which the reference pressure could be measured for the set of experiments, two longitudinal velocity distributions were obtained. One distribution was taken 7 in. below the tunnel axis (approximately the elevation of measuring section C of the model), extending from a point 6.15 diameters (50.9 in.) upstream from the axis of the model (4 in. upstream from the beginning of the working section or end of the contraction) to a point 2.40 diameters (19.9 in.) upstream from the model axis (27 in. inside the working section). The second distribution was taken at the same level but 19 in. to the right, and extended from the same point, 4 in. upstream from the beginning of the working section, to 1.68 diameters (13.9 in.) upstream from the axis of the model (33 in. inside the working section).

The two velocity distributions show an increase in velocity due to the end of the tunnel contraction followed by a plateau from about 6 in. to about 15 in. inside the working section, corresponding respectively to 4.94 and 3.85 diameters upstream from the model axis. The plateau is followed by a corresponding decrease or increase in velocity due to the presence of the model. The reference pressure for the measurements was therefore taken at a point 9 in. downstream from the end of the tunnel contraction, 19 in. to the right of the tunnel centerplane, and 6.9 in. above its floor.

C. Roughness. Two types of roughnesses were used in the present study: concentrated, in the form of longitudinal ribs, and random or uniformly distributed. The ribs were modeled by means of rectangular wires obtained commercially from the New England Wire Company with the exception of the smallest height for which cellophane tape was used. The uniformly distributed roughnesses were provided by gluing sandpaper on the

model (average grain sizes as provided by the Norton Company were 13.8x 10^{-3} in. and 2.7x10^{-3}in.; deviations from the mean are probably ± 10%). The roughness characteristics are listed in Table 2. Experiments were also run with the two "smooth" models; that is, those without any added artificial roughness except for that provided by the varnished wood of the towers, which can be considered to be at least an order of magnitude smaller than the smallest roughness relevant to this study.

As demonstrated by the dimensional analysis of the problem, the rib patterns to be investigated should allow for the systematic variation of rib height, rib width, and center-to-center spacing between ribs. The rib heights were chosen on the basis of the data available in the literature so that, with the exception of the smallest height (modeled by means of cellophane tape), the range of Reynolds number independence could be reached at Re below 500,000, the maximum attainable in the wind tunnel.

D. Mean-pressure data acquisition. The Data Acquisition and Control System (IBM 1801) of the IIHR was used to collect the mean pressure data. Figure 5 shows schematically the overall arrangement. Plastic tubes (inside diameter 0.063 in.) connect the pressure taps on the model to three different 48-terminal scanning valve connectors. Forty-six terminals were available for the pressure taps on the model; the remaining two were used for the wind tunnel reference pressures (static and total). All pressures were measured relative to the wind tunnel reference static pressure, p_o. Both reference pressures were measured by a Pitot tube installed as described in section B above. The static and total pressures were transmitted respectively to "static" and "total" chambers, from which both were recorded and the wind tunnel velocity monitored in order to ensure that each experiment was run under steady conditions.

The scanning valve connectors were connected in turn to a Scanco scanning valve, which was driven by a solenoid drive governed by a solenoid controller which could be operated either manually or automatically through the IBM 1801. In automatic operation the controller steps the scanivalve at prescribed time intervals so that each terminal is scanned in succession. The pressure at each terminal was fed to a Statham differential pressure transducer, model PM5TC, with a range of ± 0.30 psi. The signals from the pressure transducer were passed through a Dana amplifier, model 2850 V-2,

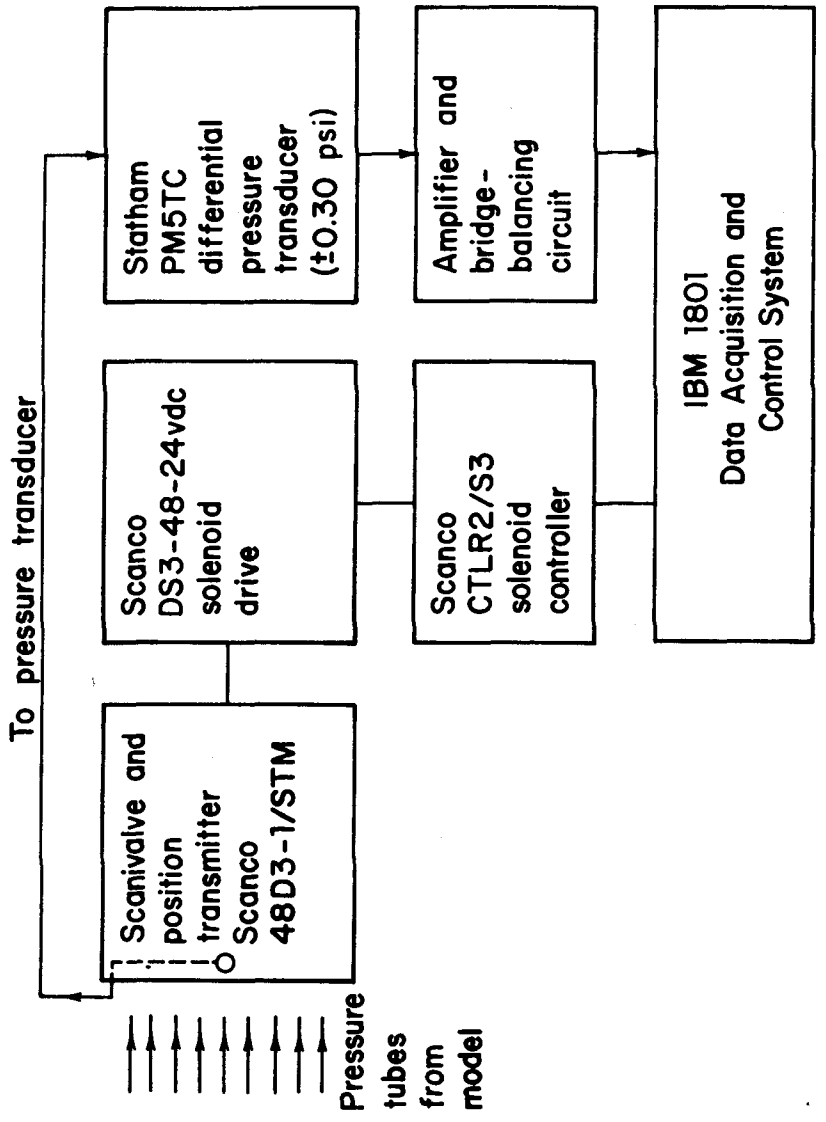

Fig. 5. Scheme of data acquisition system for the mean pressure distributions

with a low-pass filter set at 0.010 kHz bandwidth, and were then monitored, averaged, and recorded by the IBM 1801 system. The residence time for each Scanivalve port was set at 5.6 sec., with the first 0.6 sec. used to allow damping of the transients due to switching before beginning the 5-second average. (This averaging time is sufficient to eliminate the pressure fluctuations due to vortex shedding). The 0.6-second waiting time was chosen on the basis of the response of the system to a step input of pressure at a scanivalve terminal. Figure 5 provides additional information about the different units just described. The pressure data was finally obtained in the form of punched cards to be analyzed subsequently on the IBM 360/65 computer of The University of Iowa.

Before each series of experiments for a given roughness, the system was calibrated statically by applying known pressures to a scanivalve terminal and examining the (typed) output from the IBM 1801. The calibration curve was linear. In order to provide the desired calibration pressures a simple apparatus was used which consisted essentially of a flexible U-tube partially filled with water and a small-volume pressure chamber connected to one end of the U-tube. By moving the U-tube up and down the desired pressures were generated in the chamber due to the displacement of the water in the U-tube and the resulting small volume changes of the trapped air.

E. Data reduction procedure. The raw data obtained from the IBM 1801 system in the form of punched cards was subsequently analyzed on the IBM 360/65 computer of The University of Iowa Computer Center. The mean-pressure-distribution graphs obtained by means of Simplotter, a high level plotting system, have been collected in a separate appendix to this report. An interpolation mode which made use of a second degree Lagrangian interpolation polynomial to construct the curves was selected as best suited to handle the data points. For the investigations with the models with 18 and 26 ribs only the points were plotted due to the nature of the data, as explained later.

IV. RESULTS AND DISCUSSION

A. Presentation of results. Thirteen different roughness configurations were tested using the two identical models (scale 1:250) of the

hyperbolic cooling tower at Weisweiler, Germany, described earlier. To ensure that both models were identical, pressure distributions for each without any ribs were obtained. These distributions were identical within the experimental errors of the measurements. Each roughness configuration was tested at different Reynolds numbers ranging from about 1.5×10^5 to about 4.5×10^5. Except in a few cases four pressure distributions at the four levels A, B, C and D defined earlier were obtained for each Reynolds number. The pressure-measuring system was calibrated at the beginning of each series of experiments to ensure the linearity of its response. The Reynolds numbers at which tests have been carried out for each rib pattern investigated are given in Table 3.

All the mean-pressure-distribution graphs obtained by means of Simplotter have been collected in a separate (and rather lengthy) appendix to this report which can be obtained from the Institute for the cost of reproduction. The symmetry of the pressure distribution curves is in all cases excellent as can be seen in Figs. 6 and 7 where both sides of two distributions at level C, one for the smooth model and another for one of the rib configurations tested, have been plotted together with different symbols. Average mean-pressure-distributions at level C (main measuring cross section of the models), for different rib configurations and the largest Reynolds number attained in each case, are shown together in Fig. 8 for purposes of comparison.

The effect of the Reynolds number on the minimum pressure coefficient for each rib pattern is depicted in Fig. 9. Reynolds number independence is achieved in all cases for the largest Reynolds numbers investigated. Figure 9 depicts also the effect of the geometric characteristics of the different rib arrangements on the minimum pressure coefficient, to be discussed shortly. Figure 10 shows the base pressure coefficient, Cp_N (defined as the average of the wake values), plotted as a function of the Reynolds number. Again the Reynolds-number-independent range appears to have been reached for all roughness configurations with the possible exceptions of the smallest rib height ($k/d = 1.57 \times 10^{-3}$) for which a slight dependence would still seem to be present. The asymptotic values of the base pressure

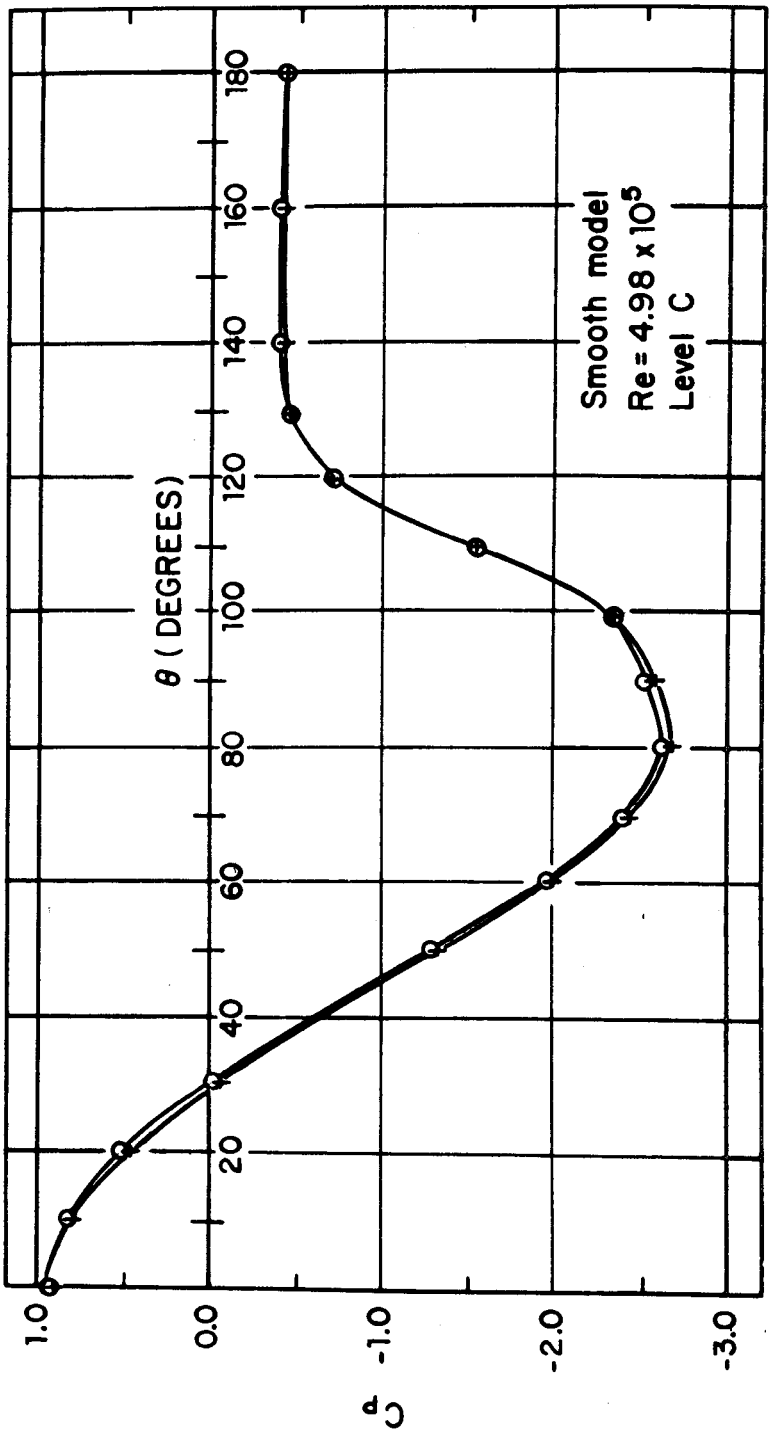

Fig. 6. Mean pressure distribution on smooth model

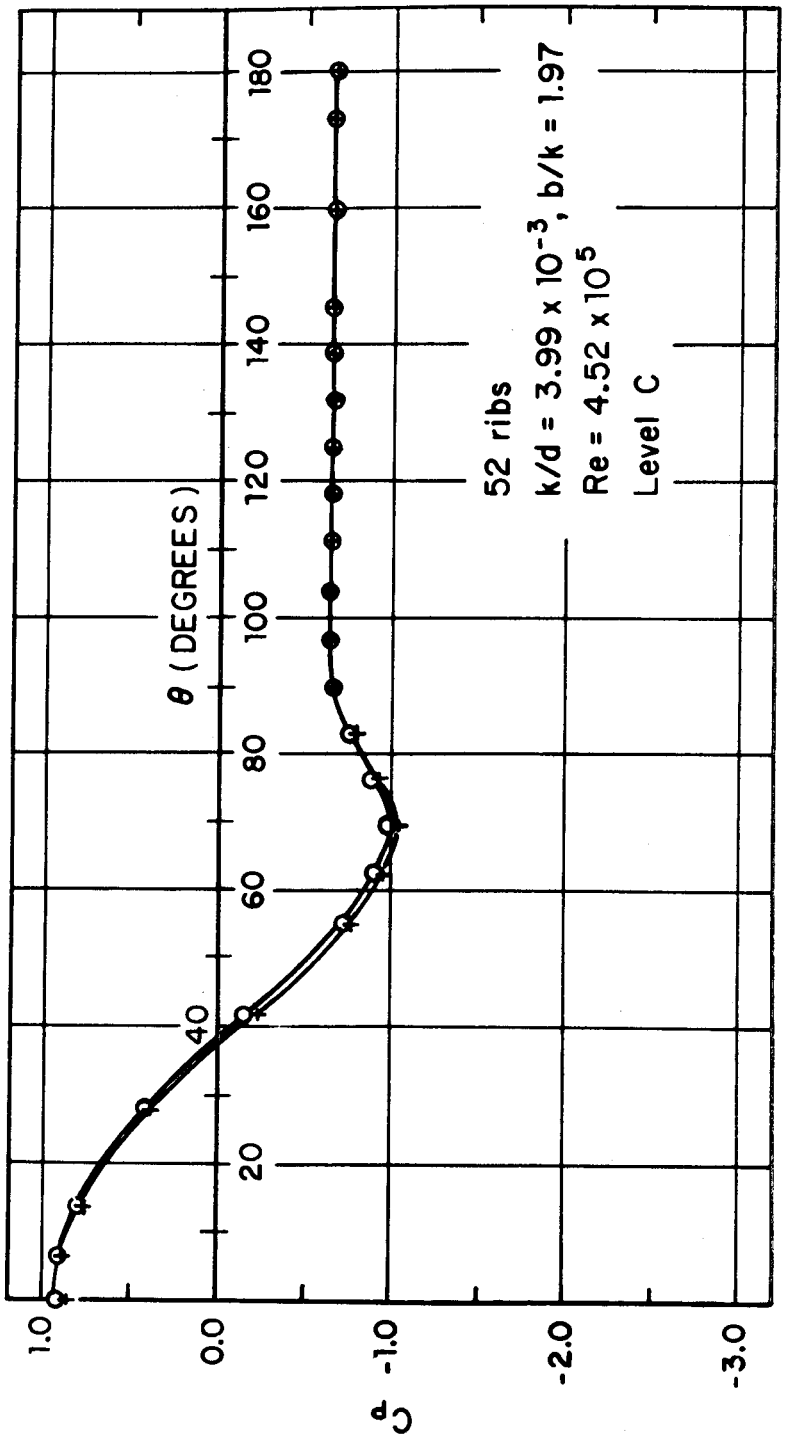

Fig. 7. Mean pressure distribution for one of the rib configurations investigated

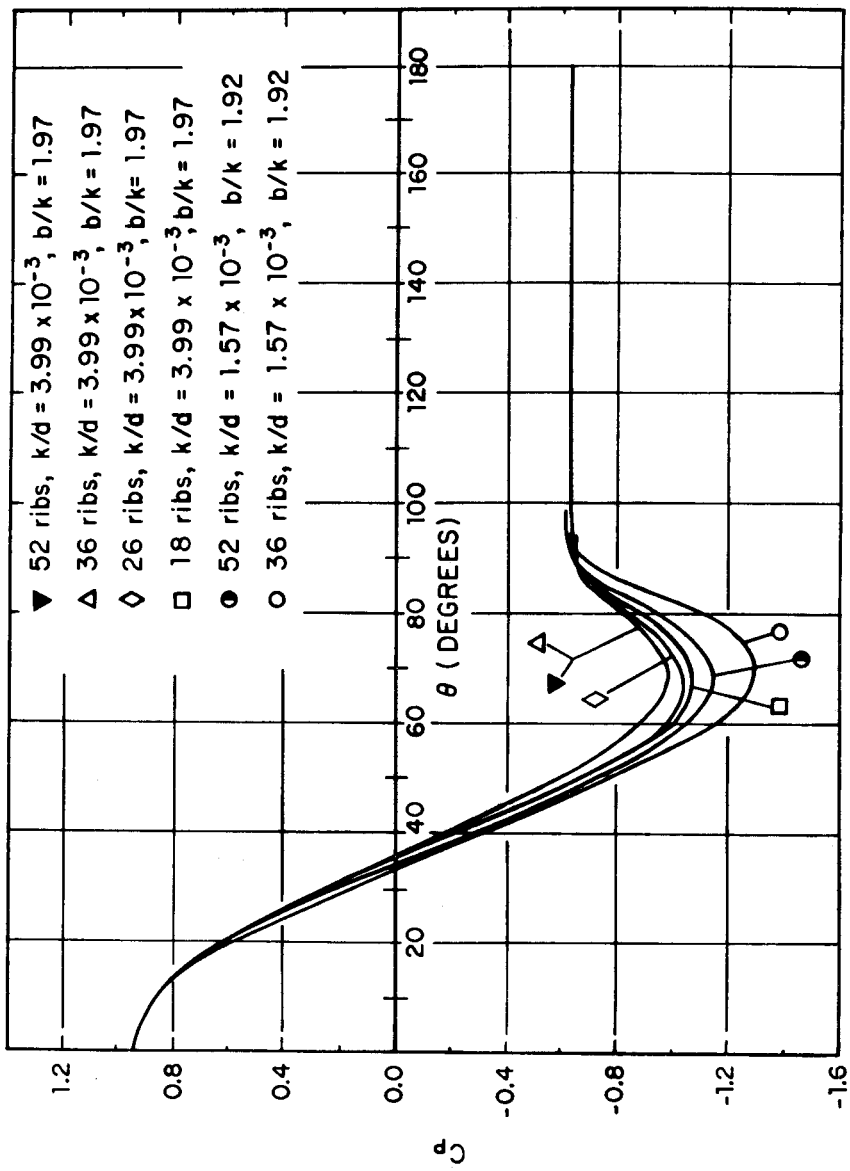

Fig. 8. Average mean pressure distributions for different roughness configurations

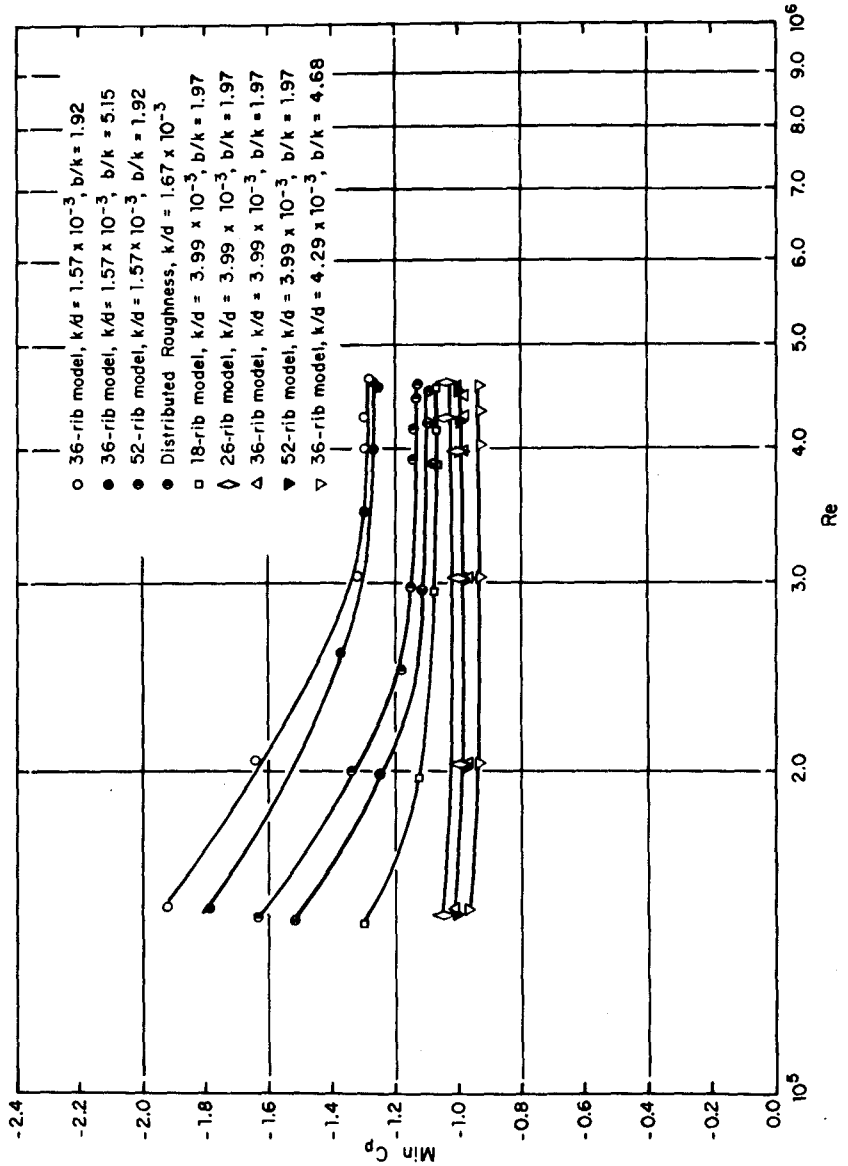

Fig. 9. Minimum pressure coefficient as a function of Reynolds number for the rib patterns investigated

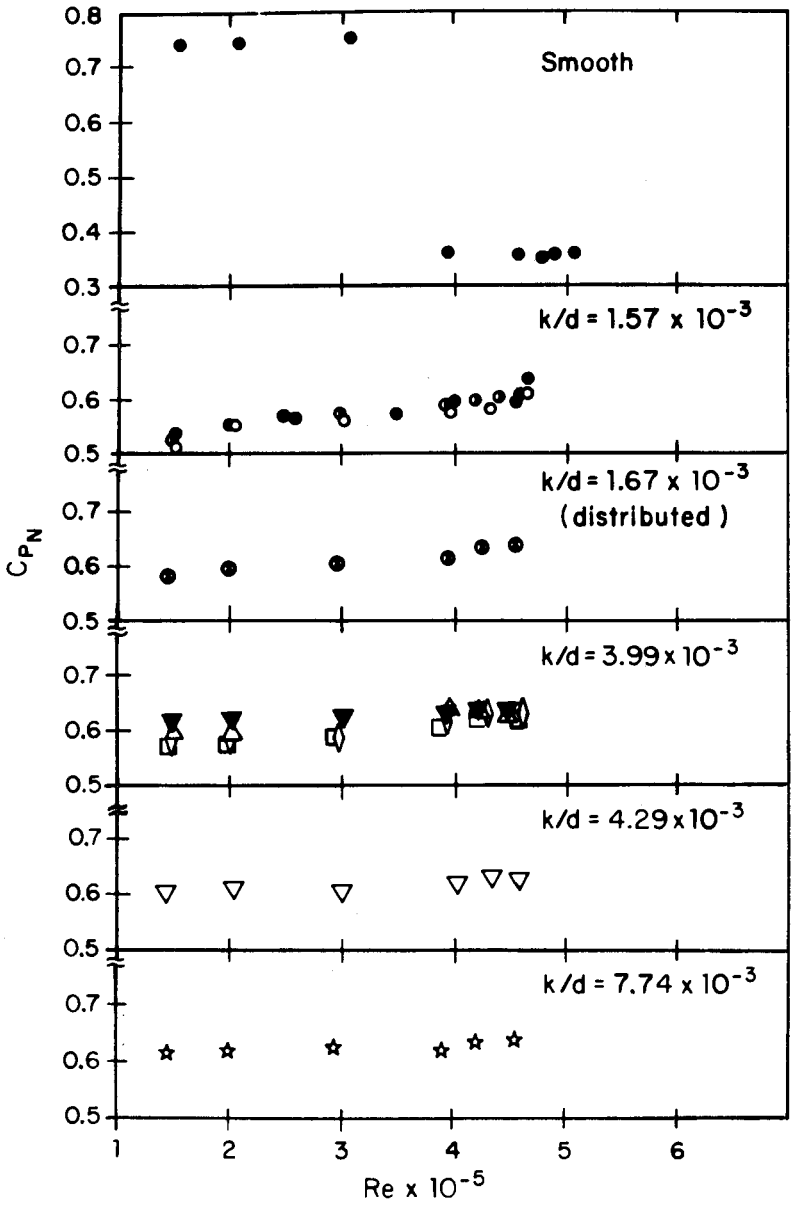

Fig. 10. Base pressure coefficient as a function of Reynolds number for the rib patterns investigated. Symbols as in Fig. 9.

coefficients are practically the same for all roughnesses, about -0.64, with the exception of $k/d = 1.57 \times 10^{-3}$ for which we have about -0.62, consistent with the slight Re dependence noted. That the base pressure coefficient is independent of the relative roughness in the range of Re independence (for large enough roughnesses) is not surprising since for structures of low aspect ratio as are those considered here the base pressure is fixed by the flow over the top of the model. This is illustrated in Figs. 11 and 12 which show that the base pressure coefficient is roughly independent of the relative height, h/H, along the tower model, whereas the minimum pressure coefficient varies with h/H. It should be noticed that, for the smooth model, the base pressure coefficient exhibits an abrupt change as the (lower or supercritical) transition in flow regimes takes place (see, e.g., Farell 1971 for a description of transitional changes with Re). The flow regime for the smooth model after the transition is still essentially different however, to the flow regime for the rough models, resulting in a smaller value of Cp_N for the smooth model due to interaction between the flows over and around the top of the tower. For the rough models, although the flow pattern changes with relative roughness (resulting in the changes in mean pressures which are the object of this study) the changes are not drastic enough (as transitional changes are) in the range of Re independence to affect the flow pattern over the top of the tower in a way that would produce a change in base pressure.

For some rib patterns (see Table 3) an additional run was carried out with air flow through the tower with mean velocity U' equal to about one fourth the free stream velocity U, at a Reynolds number larger than 4×10^5. Figures 11 and 12 show the effect of the air flow on the minimum and base pressure coefficients for the smooth model and for 9 of the roughness configurations investigated. The effect is to decrease somewhat the absolute value of the minimum pressure toward the top of the tower, and to increase it toward the bottom. The wake suction is also slightly increased. This effect, which appears to be less pronounced with increasing values of k/d, is small in all cases tested except for the smooth model, and will not be discussed further.

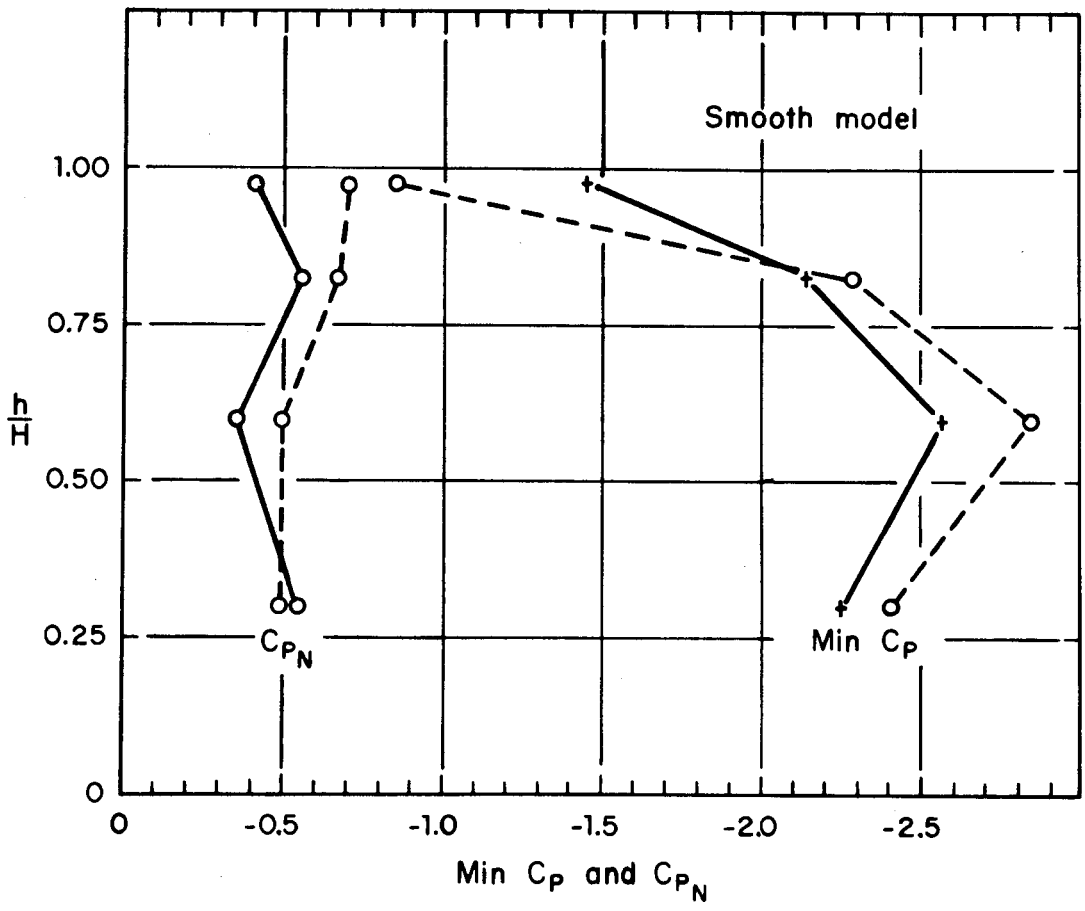

Fig. 11. Minimum and base pressure coefficients as functions of relative height along the tower for the smooth model. - - - -: with air flow through the model (U' = 0.25U), Re = 4.7×10^5; ———: without air flow through the model, Re = 4.8×10^5

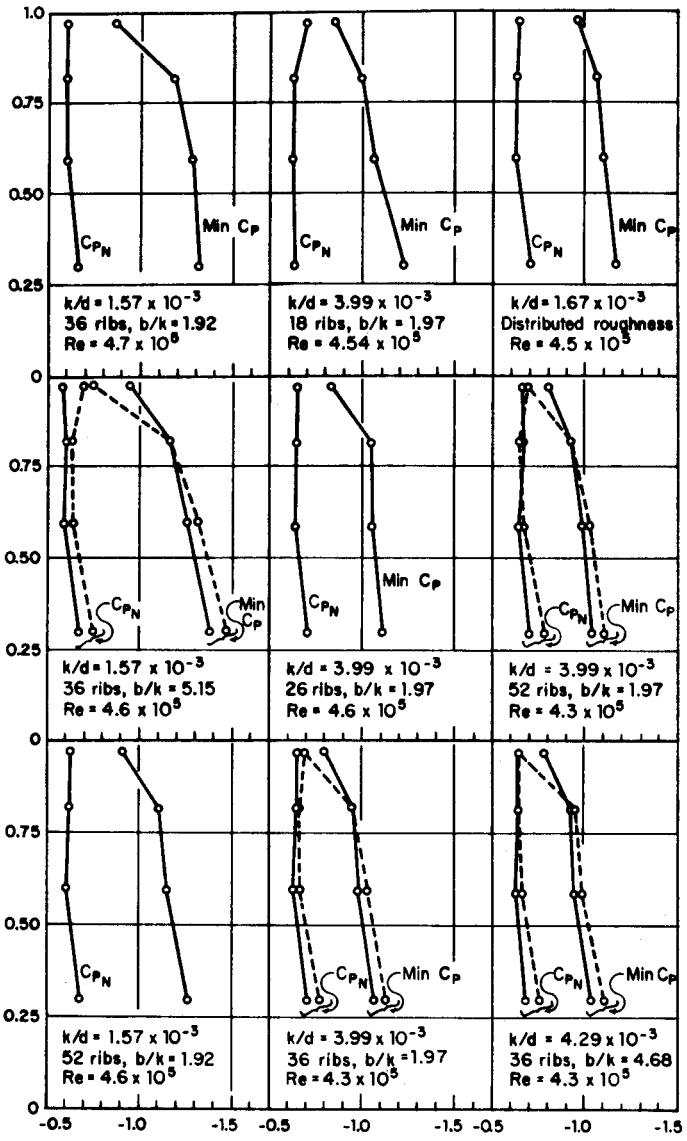

Fig. 12. Minimum and mean pressure coefficients as functions of relative height along the tower for the roughness configurations investigated. - - - -: with air flow through the model (U'/U = 0.25);————: without air flow through the model.

B. Estimate of errors in the minimum pressure coefficient due to nonuniformities in the rib height k. From the results for two of the experiments (with similar b/k ratio) with the 36-rib tower, where the minimum pressure coefficients were -1.29 for $k/d = 1.57 \times 10^{-3}$ and -0.99 for $k/d = 3.99 \times 10^{-3}$, it appears that the absolute value of min Cp decreases by about 0.01 when the value of k/d is increased by 0.08×10^{-3}. For the 52-rib tower the corresponding increase in k/d for a 0.01 reduction in the absolute value of min Cp is about 0.16×10^{-3}. Now, variations of -0.002 in. from the average size of the ribs can be expected. (Actually, variations in k of about 10% for the smaller rib sizes, and of about 8% for the larger sizes, were measured. The 0.002 in. represents an average variation for the two main rib heights tested including possible variations in the thickness of the layer of glue.) On the basis of the preceding estimates, these variations would correspond to variations in the absolute value of min Cp of 0.03 for the 36-rib model and of 0.015 for the 52-rib model. This provides an estimate of the errors in min Cp due to nonuniformities in the rib height.

C. Influence of the width-to-height ratio of the ribs. Rib types Nos. 1, 2, 3 and 4 fitted on 36-rib models were used to analyze the effect of the width-to-height ratio. For the discussion of this effect it suffices to consider the effect on min Cp, which is depicted in Fig. 9. In the zone of Reynolds number independence we have, for $k/d = 1.57 \times 10^{-3}$, min Cp = -1.29 for b/k = 1.92 and min Cp = -1.27 for b/k = 5.15. This difference in min Cp is within the experimental error. On the other hand, for $k/d = 3.99 \times 10^{-3}$ and b/k = 1.97, min Cp = -0.99, and for $k/d = 4.29 \times 10^{-3}$ and b/k = 4.68, min Cp = -0.94. In this case the values of k/d were not exactly the same, differing by 0.3×10^{-3}. As discussed in the preceding section, this difference accounts for almost 0.04 of the difference between the min Cp values, which can therefore be considered to be within the experimental error.

These results enable us to conclude that there is very little, if any, influence of the b/k ratio on the mean pressure distributions for practical values of this parameter, for which there is no interaction between the flow patterns around consecutive ribs (see sections D and E below).

D. Influence of the ratio s/k. Again it suffices to consider only the effect on min Cp. Experiments with $k/d = 1.57 \times 10^{-3}$ and $b/k = 1.92$ for $s/k = 47.6$ and $s/k = 32.6$ gave min Cp values of, respectively, -1.29 and -1.15. For $k/d = 3.99 \times 10^{-3}$ and $b/k = 1.97$, the values of min Cp were -1.07, -1.04, -0.99, and again -0.99 for s/k values of, respectively, 37.2, 25.7, 18.6, and 12.9. The results show that as expected the absolute value of min Cp decreases as the value of s/k decreases, and are in general agreement with Hayn's results, shown in Fig. 1. The effect is less pronounced for both larger values of k/d and smaller values of s/k.

Actually, for a given value of k/d, the absolute value of min Cp will eventually increase with decreasing s/k due to interaction of the flow patterns around consecutive ribs. Consider first for clarity a fixed value of b/k, say, 2, for which we have the results of the present study and also Hayn's results. If we were to plot the maximum suction values as functions of s/k for a given value of k/d, the curve would have a minimum at an optimum s/k value, and it should be relatively flat in the neighborhood of this minimum. For example, for $k/d = 3.99 \times 10^{-3}$, min Cp is the same for 52 and 36 ribs, -0.99, and the value for 26 ribs, -1.04, differs by only 5%. (The corresponding values of s/k are respectively 12.9, 18.6, and 25.7). For $k/d = 1.57 \times 10^{-3}$, there is an 11% change in the maximum suction for 36 and 52 ribs, corresponding to s/k values of 47.2 and 32.6, respectively. The optimum value of s/k is probably only slightly (if at all) dependent on k/d, since the interaction of the flow patterns around consecutive ribs depends mainly on s/k. On the basis of these and Hayn's results, for b/k of the order of 2, a value of 20 for the optimum s/k can be used as a rough approximation. (This corresponds to about 100 ribs for $k/d = 1.57 \times 10^{-3}$ and to about 40 ribs for $k/d = 4.0 \times 10^{-3}$.) Actually, because the curves are relatively flat, small departures from the optimum value should have a negligible effect on the value of min Cp.

The preceding discussion has been carried out assuming b/k constant. The optimum value of s/k must depend also on the ratio b/k. However, this dependence should be of no significance for practical applications. Indeed, curves of maximum suction versus s/k for given k/d and different

b/k ratios are coincident until interference effects appear, in accordance with the results of the preceding paragraph, and should branch off smoothly from one another when the interaction of the flow patterns around consecutive ribs begins to be felt. Since the branching off occurs near the minimum where the curves are relatively flat, although the optimum s/k may change somewhat, the actual value of the suction at this optimum value should not change significantly with b/k for small values of this parameter. In other words, the effect of a change in b/k from, say, 1 to 3, is due to the blocking of the separation region behind the upstream face of the rib by the rib itself. This effect, if at all present, is small for small b/k ratios for the case in which there is little flow pattern interaction (as the results of the preceding section show), and becomes important for values of s/k smaller than the minimum, which are not in the range of practical interest. (A smaller value of s/k implies a larger number of ribs.)

Numerical comparison of Hayn's results with the results of the present study must await development of corrections for wind tunnel blockage, which are the subject of a present study at the Institute and will be available shortly.

E. Influence of the rib height. With the 36-rib model fitted with ribs of width b=2k, min Cp = -1.29 for $k/d = 1.57 \times 10^{-3}$ and min Cp = -0.99 for $k/d = 3.99 \times 10^{-3}$. With ribs of width b=5k, a similar decrease in suction is observed. The change in min Cp for the 52-rib model is about half that for the 36-rib model. These results are in complete agreement with the general trend of Fig. 1, and we conclude that there is a marked decrease in the absolute value of min Cp when the value of k/d decreases. A comparison of all results in Fig. 1, corrected for wind-tunnel blockage, will be carried out as soon as the correction procedure presently being developed at the Institute becomes available.

As discussed in Section IV.A and depicted in Figs. 10, 11, and 12, the base pressures are fairly constant along the cooling tower height and independent of the relative roughness in the range of Reynolds number independence (that is, for large enough roughnesses). Furthermore, they are only slightly affected by air flow through the model. In other words, in the range

of Re independence, the base pressure is fixed by the flow over the top of the tower. A physical explanation for the downward trend of min Cp with increasing relative roughness can then be developed, as follows. For the flow in the boundary layer to proceed from the angle at which min Cp occurs to the angle at which separation occurs, it must negotiate a pressure increase. The ability of the flow to do so is decreased by larger roughnesses, which results in earlier separation and smaller pressure recovery in the boundary layer. Since the base pressure is fixed, the absolute value of min Cp must therefore decrease with increasing roughness. This explains the trend appearing in Fig. 1. Preliminary boundary-layer calculations in the region of the pressure increase confirm these ideas. More detailed discussion of this effect is included in publications by Farell, Carrasquel, and Güven (1974) and Farell, Maisch, and Güven (1974).

The interaction between the flow patterns around consecutive ribs discussed in the preceding section, which for closely spaced ribs may even result in stagnation regions being formed between ribs which clearly reduce the effectiveness of the rib action was observed in experiments with the 36-rib model with $k/d = 7.74 \times 10^{-3}$ and $b/k = 2.05$, for which min Cp was about -1.01. This slight increase in the absolute value of min Cp with respect to the value of -0.99 corresponding to $k/d = 3.99 \times 10^{-3}$ (and to that of -0.94 corresponding to $k/d = 4.29 \times 10^{-3}$) confirms results for large roughnesses obtained by Pris (1961) and Niemann (1971). The effect of the interaction is to reduce the effective height of the rib, and should thus be avoided.

F. Comparison of results of the present study with results obtained by Niemann (1971). Niemann (1971) made experiments on a 1:200 scale model of the same cooling tower, analyzing the effect of relative roughness over a similar range of values of k/d for models with 52 ribs. His results, summarized in the literature review and represented in Fig. 1, follow trends similar to those of the present study. Niemann's absolute values for min Cp in the range of Reynolds number independence are lower, however, than those presented here. This difference is very likely due to his much lower blockage ratio, numerical comparison with his results requires application of a correction procedure for wind tunnel blockage; this is accomplished by Farell, Carrasquel, and Güven (1974).

Both Niemann's and the present results for the 52-rib models are shown in Fig. 13, in which min Cp is plotted as a function of Reynolds number

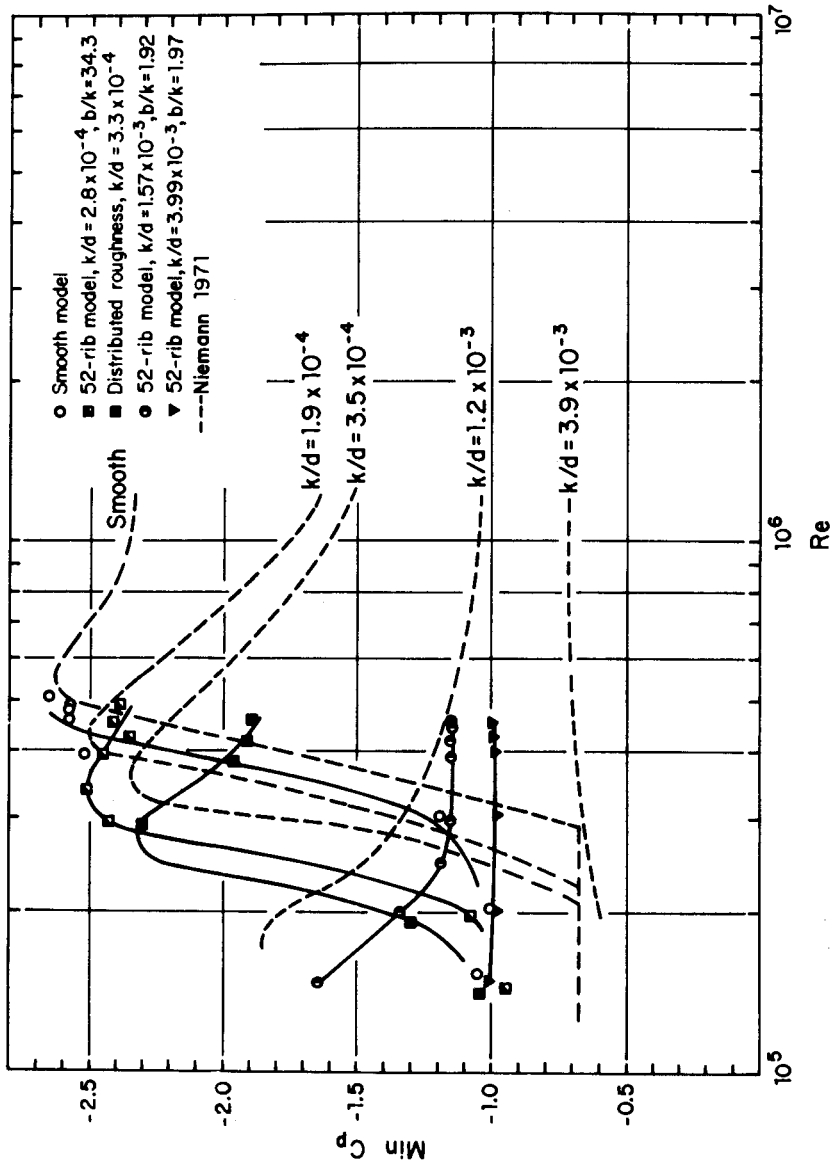

Fig. 13. Comparison of Niemann's results (in dashed lines) with results obtained in the present study. (Results for ribbed models are for 52 ribs.)

for different k/d values. Shown also in this figure for purposes of comparison are the results for the smooth models and for the two smallest roughnesses investigated, $k/d = 2.8 \times 10^{-4}$ (cellophane tape) and $k/d = 3.3 \times 10^{-4}$ (distributed). Niemann's curves are shown as dashed lines; the point corresponding to his prototype measurements, for which min Cp = -1.30 for $k/d = 3.5 \times 10^{-4}$ and $Re > 4.5 \times 10^{7}$, is not shown.

It should be noted that in both Niemann's and the present investigation independence of the Reynolds number was achieved in the model experiments with the larger roughnesses, as depicted in Figs. 9 and 13. Once Re independence is achieved no changes in min Cp should occur for larger Reynolds numbers, and the model results are under these conditions applicable to prototype structures.

G. Comparison of the effect of concentrated and distributed roughnesses. The model with 138 pressure taps was tested with two distributed or random roughnesses, with k/d values of 1.67×10^{-3} and 3.3×10^{-4}. The value of k was estimated on the basis of data supplied by the sandpaper manufacturer; deviations from the mean are probably of the order of $\pm$ 10%. The purpose of these tests was to compare the effects of distributed and rib roughnesses.

For $k/d = 1.67 \times 10^{-3}$, min Cp = -1.10 in the range of Reynolds number independence (see Fig. 9). The result is somewhat smaller than that for the 52-rib model with $k/d = 1.57 \times 10^{-3}$ (min Cp = -1.15). But the difference is not large and may be considered to be within the experimental accuracy if account is taken of the difference in the k/d values as done earlier in the discussion of the effect of b/k. This excellent agreement is, in a way, somewhat surprising. Indeed, although we have comparable k/d values in both cases, for the rib roughness k is the rib height, while for the distributed or random roughness k is the average grain diameter as given by the manufacturer (no information is available on size distribution and packing of the grains).

For $k/d = 3.3 \times 10^{-4}$, the results show (see Fig. 13) that the range of Reynolds number independence has not been reached. The closest relative rib height tested is $k/d = 2.8 \times 10^{-4}$, obtained using cellophane tape (for which the results are also in the range of Re dependence). The measured

absolute thickness of the cellophane tape was actually only 0.0023 in., a very small value difficult to measure accurately. Furthermore, because of the small thickness involved, the effective height of the cellophane-tape rib on the model may be somewhat different from the measuredthickness of the tape. If one considers in addition the uncertainty in the value of k for the random roughness, the curves for $k/d = 2.8 \times 10^{-4}$ and $k/d = 3.3 \times 10^{-4}$ in Fig. 13 (both in the range of Reynolds number dependence) can be considered to be in general agreement, in particular because transitional changes with Reynolds number are rather sensitive to changes in the roughness configuration.

Similar remarks can be made about Niemann's results for the smaller roughnesses. A comparison of Niemann's and the present results after correction for blockage effects is given by Farell, Carrasquel, and Güven (1974).

In conclusion, subject to the considerations in this section, the results of the tests with the two distributed roughnesses indicate that this type of roughness has an effect very similar to that of concentrated or rib roughness. Accurate quantitative agreement between both roughness types may depend on a correct geometric characterization of the distributed or random roughness. A comparison of the effect of both roughness types on the pressure fluctuations on the structure (including crisscross and staggered rib patterns would be of immediate interest.

H. Interference effects between ribs and pressure taps. The experiments for 26 and 18 ribs were performed with the model towers used respectively for 52 and 36 ribs. Consequently, the pressure taps for these experiments were not midway between ribs but at distances 0.25s from them. The pressure taps immediately upstream from the ribs detected pressures higher than those obtained by interpolation of the readings corresponding to the pressure taps immediately downstream from them. This is due to the stagnation effect on the flow upstream from a rib and the separation zone downstream from it. For the model tower with 18 ribs the minimum pressure coefficients obtained on the basis of the readings upstream from the ribs were about 9% higher than those corresponding to the readings downstream from them. For the model tower with 26 ribs this difference was larger (about 18%)

because the ribs were closer to the pressure taps. The minimum pressure coefficients given in Fig. 9 are averages of the upstream and downstream readings.

The experiments for 26 and 18 ribs provided indirectly an evaluation of the effect of a wind stream striking the tower from a direction not in a plane of symmetry of the rib configuration (that is, with the stagnation point at distances 0.25s and 0.75s from the two immediate ribs). For the model with 18 ribs an asymmetry of about 7.5% was observed. This asymmetry is very likely due to the different location of the ribs on both sides of the tower relative to the stagnation point which results in a different effect upon the early boundary layer development. (Actually, these results show that the "early boundary layer" is really a collection of stagnation regions and separation pockets.) For the model with 26 ribs, the asymmetry was within the experimental error.

In both cases the minimum pressure coefficients reported are obtained as averages of the values for both sides of the model.

J. Characterization of a pressure distribution. Niemann (1971) suggests that the pressure distribution in the middle third of a cooling tower can be characterized by a number of parameters, namely, the largest pressure coefficient, max Cp, the position of the zero-crossing of the pressure distribution, θ_0, the minimum pressure coefficient, min Cp, its position, θ_1, and, finally, the magnitude of the wake suction, Cp_N, and the beginning of the wake region, θ_N. The angles given are relative to the position of the stagnation point, taken as origin. The maximum pressure is nearly equal to the stagnation pressure and max Cp is therefore nearly equal to one.

These parameters can be accurately determined from the pressure distributions with the exception of the beginning of the wake region, which is not marked by an angular point as the measurements have shown. Rather, the mean pressure gradient changes continuously near separation. (The experimental determination of the point of separation for the mean flow about these structures is difficult on account of the fluctuating nature of the actual flow.) The beginning of the wake region is defined here, following Niemann,

because the ribs were closer to the pressure taps. The minimum pressure coefficients given in Fig. 9 are averages of the upstream and downstream readings.

The experiments for 26 and 18 ribs provided indirectly an evaluation of the effect of a wind stream striking the tower from a direction not in a plane of symmetry of the rib configuration (that is, with the stagnation point at distances 0.25s and 0.75s from the two immediate ribs). For the model with 18 ribs an asymmetry of about 7.5% was observed. This asymmetry is very likely due to the different location of the ribs on both sides of the tower relative to the stagnation point which results in a different effect upon the early boundary layer development. (Actually, these results show that the "early boundary layer" is really a collection of stagnation regions and separation pockets.) For the model with 26 ribs, the asymmetry was within the experimental error.

In both cases the minimum pressure coefficients reported are obtained as averages of the values for both sides of the model.

J. Characterization of a pressure distribution. Niemann (1971) suggests that the pressure distribution in the middle third of a cooling tower can be characterized by a number of parameters, namely, the largest pressure coefficient, max Cp, the position of the zero-crossing of the pressure distribution, θ_0, the minimum pressure coefficient, min Cp, its position, θ_1, and, finally, the magnitude of the wake suction, Cp_N, and the beginning of the wake region, θ_N. The angles given are relative to the position of the stagnation point, taken as origin. The maximum pressure is nearly equal to the stagnation pressure and max Cp is therefore nearly equal to one.

These parameters can be accurately determined from the pressure distributions with the exception of the beginning of the wake region, which is not marked by an angular point as the measurements have shown. Rather, the mean pressure gradient changes continuously near separation. (The experimental determination of the point of separation for the mean flow about these structures is difficult on account of the fluctuating nature of the actual flow.) The beginning of the wake region is defined here, following Niemann,

as the point of intersection of the tangent with the contact of the highest order in the region of the pressure increase behind the minimum, and the parallel to the θ-axis determined by Cp_N.

In this manner one obtains five parameters corresponding to key supporting points of a mean-pressure distribution curve which, together with an assumption about the trend of the individual curve sections between the supporting points, may be used to describe the given pressure distribution. In order not to have to pursue individually the influence of Re and k/d on the five parameters, we examine here whether the different pressure distributions show certain general regularity resulting in correlations of the various parameters defined above with min Cp, as suggested by Niemann (1971).

In Fig. 14 the correlation between the position of the zero-crossing, θ_o, and the pressure minimum is depicted on the basis of the results of the present experiments. The points shown correspond to section C of the models and to all tests listed in Table A-3 on lines 3 through 7, excluding those with air flow through the model. The points corresponding to the three largest Re for the smooth model are also shown. For the model with the cellophane tape ribs and the three largest Re investigated, the values of min Cp are -2.35, -2.41, and -2.39, with corresponding values of the angle θ_o all the same and equal to 29 deg. (These three points were not plotted but confirm the general trend.) The scatter in Fig. 14 is somewhat larger than the scatter in Niemann's corresponding plot. The difference with the curve obtained by Niemann, shown as a dashed line, might be partially due to blockage effects.

Figure 15 shows a similar correlation between the pressure minimum and its position, θ_1. The plotted points correspond to the points in Fig. 14; for the model with the cellophane-tape ribs we have θ_1 values of 79 deg., 82 deg., and 80 deg., respectively, for the min Cp values given in the preceding paragraph. (Again these points were not plotted but confirm the general trend.) As for Fig. 14, the scatter is somewhat larger than that in Niemann's corresponding plot, and there is a difference in the resulting mean curves.

Finally, Fig. 16 shows a similar correlation for the beginning of the wake region. Following Niemann, the correlation presented is between

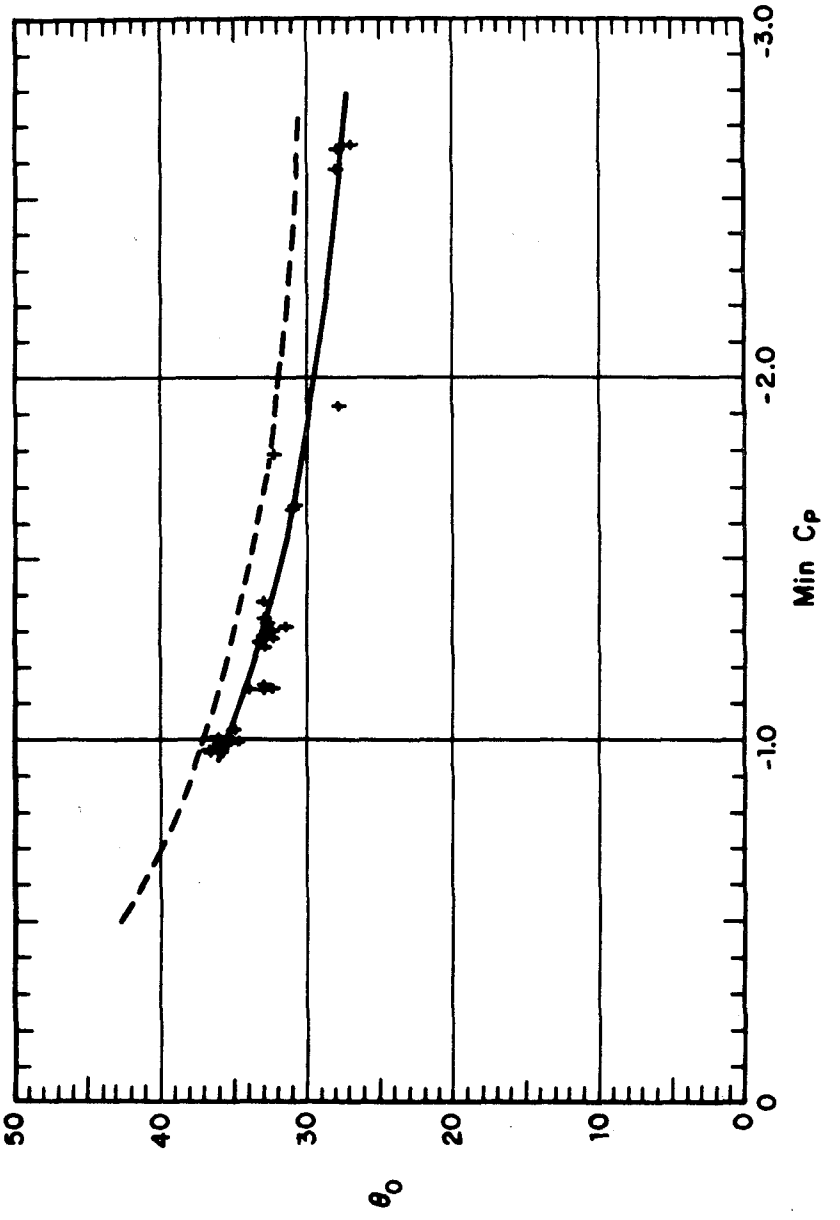

Fig. 14. Zero crossing of the pressure distribution as a function of the pressure minimum. - - - -: Niemann (1971)

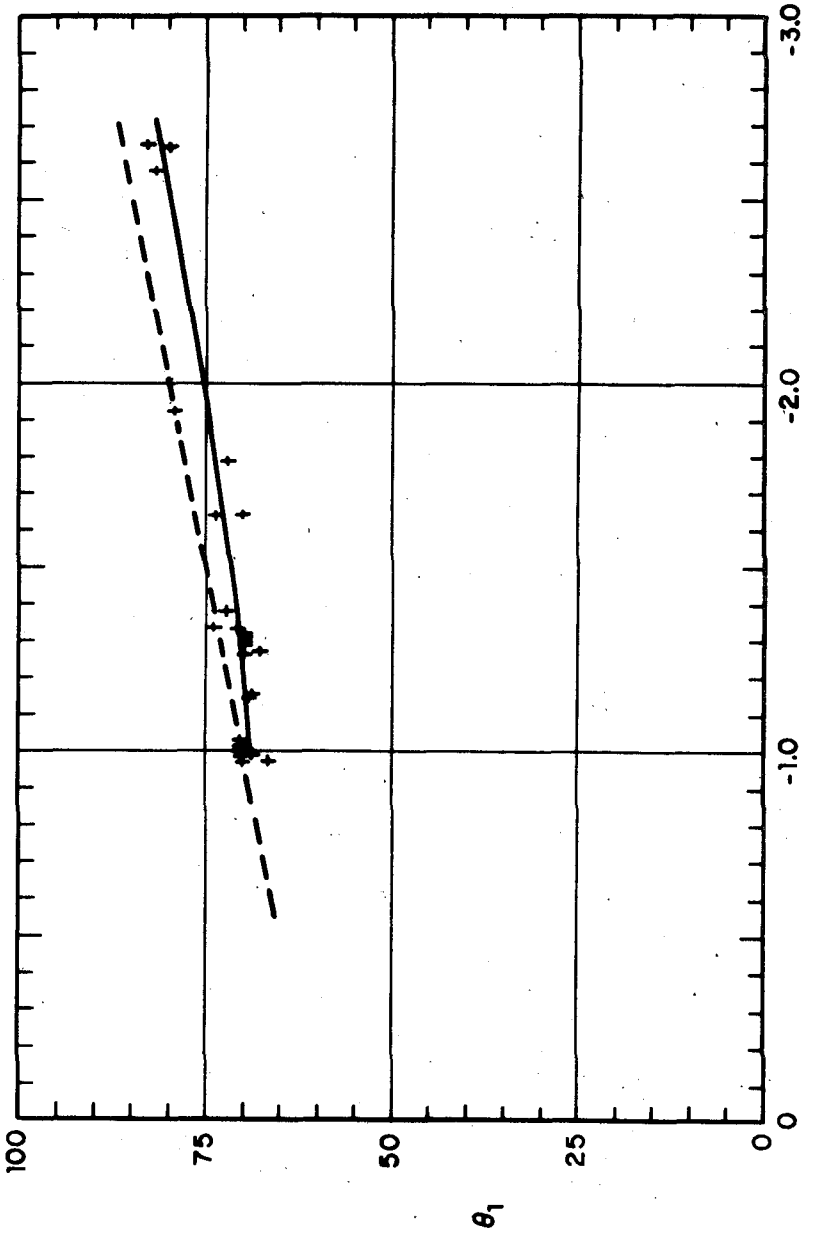

Fig. 15. Correlation between position of the pressure minimum and its magnitude. - - - -: Niemann (1971)

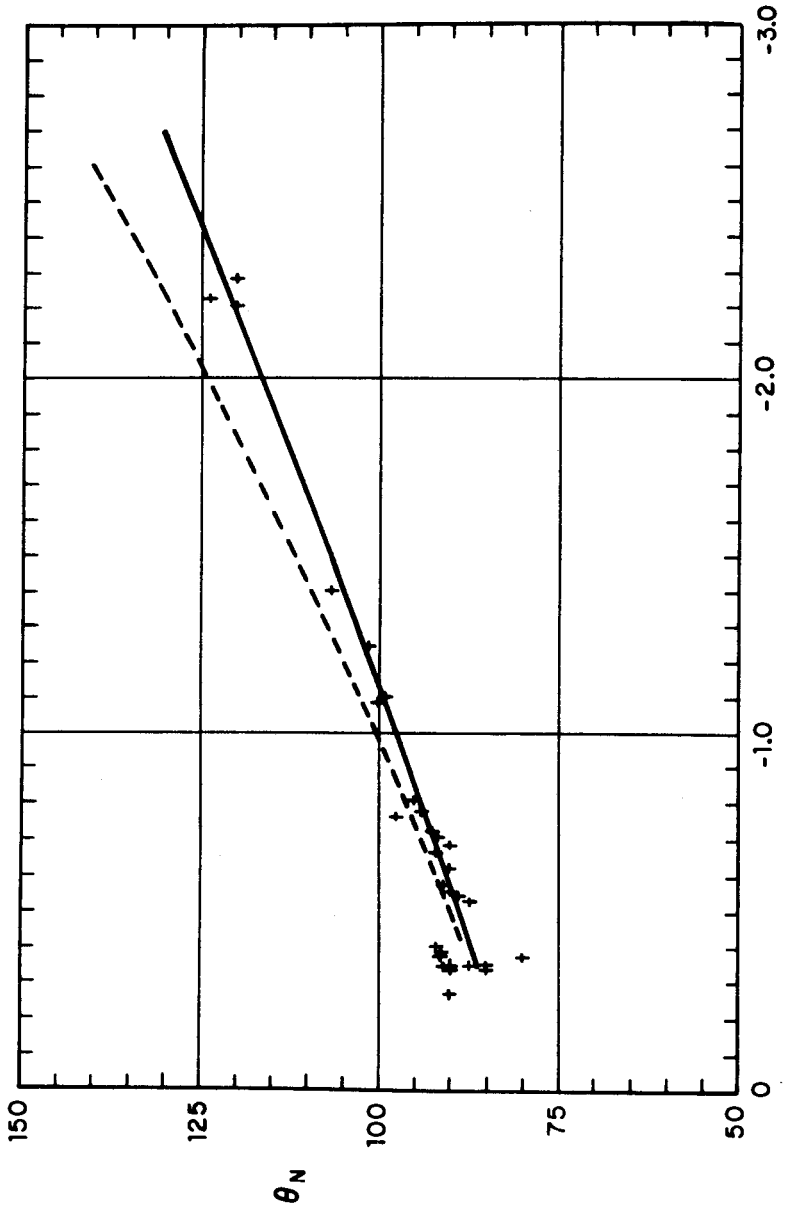

Fig. 16. Correlation between beginning of dead water region, θ_N, and pressure-distribution characteristic value min Cp - Cp_N. - - - -: Niemann (1971)

θ_N and min Cp - Cp_N. Some justification for this correlation can be found in the discussion in section IV.E. The points shown correspond again to the points in Fig. 14; for the model with the cellophane-tape ribs we have θ_N values of 115 deg., 116 deg., and 115 deg., respectively, for values of min Cp-Cp_N of -1.95, -1.99, and again -1.95, corresponding to the same three experiments of the two preceeding paragraphs. (Again these points were not plotted but confirm the general trend.) The scatter is now somewhat larger than that in Figs. 14 and 15, and larger also than the scatter in Niemann's corresponding plot. Again there is a difference with Niemann's curve, shown as a dashed line.

The results of this section tend to confirm that, at least in first approximation, it is possible to describe as suggested by Niemann the pressure distribution in the middle third of a cooling tower by only one characteristic value, min Cp. (The base-pressure coefficient, Cp_N, is fixed by the flow over the top of the tower in the range of Reynolds number independence, and is therefore independent of the relative roughness.) The scatter in the present results is larger however than that in Niemann's plots, and there is some difference in the resulting mean correlation curves, which might be due in part to blockage effects.

V. CONCLUSIONS

The primary purpose of the present study was to investigate the effect of external, concentrated roughness elements or ribs on the mean pressure distributions on model hyperbolic cooling towers in uniform wind, in the region of Reynolds number independence. Several longitudinal rib configurations were tested, systematically varying rib height, rib width, and rib spacing. Two uniformly distributed, or random, roughnesses were also tested for purposes of comparison. The main results of the study are briefly summarized below. It should be noted that in both Niemann's (1971) and the present investigations independence of the Reynolds number was achieved in the model experiments with the larger roughnesses, as depicted in Figs. 9 and 13. Once Re independence is achieved no changes in

min Cp should occur for larger Reynolds number, and under these conditions the model results are applicable to prototype structures.

The base pressure coefficient, Cp_N, is fairly constant along the height of the cooling tower model and, in the range of Reynolds number independence, it is fixed by the flow over the top of the tower. That is, although the flow pattern changes with relative roughness (resulting in the changes in mean pressure that are the object of this study) the base pressure coefficient does not. On the other hand, the difference between the absolute values of the minimum and base pressure coefficients, min $Cp - Cp_N$, decreases with increasing relative roughness, k/d, if there is no interaction between the flow patterns around consecutive ribs. Therefore, under these conditions, an increase in relative roughness results in a reduction in the magnitude of the negative pressures on the sides of the model.

This reduction in mean suction with increasing relative roughness is significant. For example, for the 36-rib model fitted with ribs of width b = 2K, min Cp decreases from -1.29 for $k/d = 1.57 \times 10^{-3}$ to -0.99 for $k/d = 3.99 \times 10^{-3}$. The corresponding change in min Cp for the 52-rib model was about half that for the 36-rib model. These results are in complete agreement with the general trend of the available data, depicted in Fig. 1. A full numerical comparison of available results after a tunnel-blockage correction procedure is applied is presented by Farell, Carrasquel, and Güven (1974).

The width-to-height ratio of the ribs, b/k, has very little, if any, influence on the mean pressure distributions for practical values of this parameter, for which there is no interaction between the flow patterns around consecutive ribs. On the other hand, the reductions in mean suction depend as expected on the relative rib spacing, s/k. For example, for b/k equal to about 2 and $k/d = 1.57 \times 10^{-3}$, we have min Cp = -1.29 for s/k = 47.6 and min Cp = -1.15 for s/k = 32.6. Actually, for a given k/d, min Cp decreases first and then increases as the value of s/k decreases. The increase is due to interference effects between the flow patterns around consecutive ribs. The optimum value of s/k (excluding considerations of cost) corresponds to the minimum value of min Cp and is probably only slightly

(if at all) dependent on k/d, since the interaction of the flow patterns around consecutive ribs depends mainly on s/k. On the basis of these and Hayn's (1967) results, for b/k of the order of 2, a value of 20 for the optimum s/k can be used as a rough approximation. (This corresponds to about 100 ribs for $k/d = 1.57 \times 10^{-3}$ and to about 40 ribs for $k/d = 4.0 \times 10^{-3}$.) Actually, because the curves are relatively flat in the neighborhood of the minimum, small departures from the optimum value should have a negligible effect on the resulting value of min Cp.

The results of tests with two distributed roughnesses indicate that this type of roughness has an effect very similar to that of concentrated or rib roughness. Accurate quantitative agreement between both roughness types may depend on a correct geometric characterization of the distributed or random roughness. A comparison of the effect of both roughness types on the pressure fluctuations on the structure (including crisscross and staggered rib patterns) would be of immediate interest.

Finally, the results of the study tend to confirm that, at least in first approximation, it is possible to describe the pressure distribution in the middle third of a cooling tower by only one characteristic value, min Cp, as suggested by Niemann. The scatter in the correlations (on which this conclusion is based) among the various parameters describing the pressure distribution curves is larger, however, than the scatter in Niemann's corresponding plots, and there is some difference in the resulting mean correlation curves, which might be due in part to blockage effects.

REFERENCES

1. Armitt, J. (1968) "The effect of surface roughness and free stream turbulence on the flow around a model cooling tower at critical Reynolds numbers," Proceedings of a Symposium on Wind Effects on Buildings and Structures, Loughborough University of Technology, England.

2. Cowdrey, C.F., and O'Neill, P.G.G. (1956) "Reports of tests on a model cooling tower for the C.E.A. Pressure measurements at high Reynolds numbers," National Physical Laboratory, NPL/Aero/316a.

3. Davenport, A.G., and Isyumov, N. (1966) "The dynamic and static action of wind on hyperbolic cooling towers," University of Western Ontario, Canada, Engineering Science Research Report, BLWT-1-66.

4. Dryden, H.L., and Hill, G.C. (1930) "Wind pressure on circular cylinders and chimneys," U.S. Bureau of Standards, Journal of Research, Vol. 5, pp. 653-693.

5. Ebner, H. (1968) "Untersuchung des Einflusses der Kraftwerksgebäude auf die Windbelastung des Balcke-Naturzugkühlturms Kraftwerk Mengede (GBAG)," Technische Hochschule Aachen,Lehrstuhl für Leichtbau, Bericht Nr. 21/1968.

6. Farell, C. (1971) "On the modeling of wind loading on large cooling towers," Proceedings, Second Annual Thermal Power Conference and Fifth Biennial Hydraulics Conference, Washington State University, Pullman, Washington, pp. 139-166.

7. Farell, C., Carrasquel, S., and Güven. O. (1974 "Effects of wind tunnel walls on flows about circular cylinders and model hyperbolic cooling towers," journal article in preparation at the Iowa Institute of Hydraulic Research, The University of Iowa, Iowa City.

8. Farell, C., Maisch, F., and Güven, O (1974), "Surface roughness effects on the mean wind pressure distribution on hyperbolic cooling towers," journal article in preparation at the Iowa Institute of Hydraulic Research, The University of Iowa, Iowa City.

9. Golubovic, G. (1957) "Etude aérodynamique d'une tour réfrigérante en forme d'hyperboloide de révolution," Pub. Int. Ass. Br. and Str. Eng., Vol. 17, pp. 87-94.

10. Hayn, F. (1967) "Druckverteilungsmessungen am Modell des Kraftwerks Scholven," Deutsche Versuchsanstalt für Luft-und Raumfahrt E.V., Institut für angewandte Gasdynamik, Port-Wahn, Bericht AM 511.

11. Kennedy, J.F. (1971) "Wet cooling towers," MIT Short Course on Engineering Aspect of Heat Disposal from Power Generation, Cambridge, Massachusetts.

12. Niemann, H.J. (1971) "On the stationary wind loading of axisymmetric structures in the transcritical Reynolds number region," Institut für Konstruktiven Ingenieurbau, Ruhr-Universität Bochum, Report No. 71-2.

13. Paduart, A. (1968) "Stabilité des tours de réfrigération," Le Genie Civil, Vol. 145, No. 2, pp. 100-112.

14. Pris, M.R. (1959) "Etudes aérodynamiques I: Tour de refrigeration hyperbolique," Annales de l'Institute Technique du Bâtiment et des Travaux Publics, No. 134, pp. 147-167.

15. Pris, M.R. (1961) "Etudes aérodynamiques IV: Réservoirs et cheminées. Résistance de cylindres á base ploygonale a arétes vives ou munis de nervures. Résistance de cylindres a base circulaire et a surface rugueuse," Annales de l'Institut Technique du Bâtiment et des Travaux Publics, Nos. 163-164, pp. 736-756.

16. Rogers, P., and Cohen, E.W. (1970) "Hyperbolic cooling towers, development and practice," Journal of the Power Division, ASCE.

17. Shaw, R. (1960) "The influence of hole dimensions on static pressure measurements," J. Fluid Mech., Vol. 7, pp. 550-564.

APPENDIX A = TABLES

Table A-1

Literature review

Author	Niemann 1971	Niemann 1971	Present study	Hayn 1967
Experimental Model	Weisweiler cooling tower (prototype)	Model of Weisweiler tower	Model of Weisweiler tower	Model of Scholven cooling tower (shape similar to Weisweiler tower)
Roughness	Longitudinal ribs	Longitudinal ribs	Longitudinal ribs	Longitudinal ribs
H/d	2.0	2.0	2.0	2.28
ℓ_1/d	0.52	0.52	0.52	0.47
ℓ_2/d	0.81	0.70	0.81	0.80
Horizontal blockage (%)	Prototype	3.7	13.8	6.2
Vertical blockage (%)	Prototype	12.7	50.4	25.2
Reynolds number	$> 4.5 \times 10^7$	1.2×10^6	4.5×10^5	9.6×10^5

Table A-1 (cont'd)

Author	Ebner 1968	Golubovic 1957	Golubovic 1957	Pris 1961
Experimental model	Model of Mengede cooling tower (shape more like a cylinder)			Cylinder, suspended
Roughness	Longitudinal ribs	Longitudinal ribs	Crisscross rib pattern	Longitudinal ribs
H/d	1.93	2.05	2.05	1.33
ℓ_1/d	0.41	0.66	0.66	
ℓ_2/d	1.08			0.67
Horizontal blockage (%)	19.2			15.0
Vertical blockage (%)	54.0			20.0
Reynolds number	6.4×10^5	10^5	10^5	6.0×10^5

Table A-1 (cont'd)

Author	Pris 1961	Pris 1961	Cowdrey and O'Neill 1956	Armitt 1968
Experimental model	Cylinder, suspended	Hyperbolic cooling tower model (shape: fairly wide toward the bottom)	Model of cooling tower (shape: cylindrical throat and two truncated cones)	Model of cooling tower (shape: same as Cowdrey and O'Neill's model)
Roughness	Longitudinal ribs	Distributed	Distributed	Distributed
H/d	4	1.55	1.80	1.80
ℓ_1/d		0.10	0.38	0.38
ℓ_2/d	2.0	0.29	0.57	0.57
Horizontal blockage (%)	7.5	17.0	20.8	8.3
Vertical blockage (%)	30.0	35.0	40.9	43.6
Reynolds number	3.0×10^5	6.4×10^5	9.3×10^6 14.1×10^6	4.9×10^5

Table A-1 (cont'd)

Author	Dryden and Hill 1930	Davenport and Isyumov 1966
Experimental model	Prototype stack (circular cylinder)	Model of Fort Martin cooling tower (shape similar to Weisweiler tower)
Roughness	Distributed	Distributed
H/d	3	1.86
ℓ_1/d		0.25
ℓ_2/d	1.00	0.81
Horizontal blockage (%)	Prototype	8.4
Vertical blockage (%)	Prototype	18.0
Reynolds number	2.5×10^6 to 4.7×10^6	1.55×10^5

Table A-2

Roughness characteristics

Rib type number or roughness type	k (in.)	b (in.)	$k/dx10^3$	b/k
0	0.0	0.0	0.0	-
1	0.013	0.025	1.57	1.92
2	0.013	0.067	1.57	5.15
3	0.033	0.065	3.99	1.97
4	0.0355	0.166	4.29	4.68
5	0.064	0.131	7.74	2.05
Cellophane tape	0.0023	0.079	0.28	34.3
Distributed roughness	0.0138	-	1.67	-
Distributed roughness	0.0027	-	0.33	-

k = average rib height (including thickness of the layer of glue of 0.0008 in.) or average grain size

b = average rib width

c = model mean diameter = 8.27 in.

Table A-3

Summary of tests

Number of ribs	Rib type number	Reynolds number x 10^{-5}								
36	0	4.98								
52	0	1.53	2.05	3.05	3.94	4.58	4.78	4.87	5.06	4.71*
36	1	1.49	2.04	3.04	3.99	4.27	4.65			
52	1	1.47	2.00	2.49	2.97	3.91	4.20	4.42	4.58	
36	2	1.49	2.57	3.49	3.98	4.55	4.61			4.55*
36	3	1.49	2.03	3.03	3.96	4.28	4.48			4.25*
52	3	1.48	2.02	3.03	3.97	4.24	4.52			4.19*
36	4	1.48	2.03	3.04	4.01	4.33	4.56			4.34*
36	5	1.44	1.97	2.95	3.90	4.23	4.55			
18	3	1.44	1.97	2.94	3.86	4.20	4.54			
26	3	1.46	2.03	3.02	3.96	4.28	4.61			
52	cellophane tape	1.45	1.98	2.98	3.39	3.93	4.28	4.55	4.88	
Distributed roughness	k/d = 1.67×10^{-3}	1.45	1.98	2.95	3.88	4.25	4.53			
Distributed roughness	k/d = 3.3×10^{-4}	1.41	1.94	2.90	3.82	4.19	4.59			

*with air flow through the tower